AD-A068 265 OAKLAND UNIV ROCHESTER MICH SCHOOL OF ENGINEERING F/G 11/3
DETERMINATION OF STRAINS IN PHOTOELASTIC COATINGS,(U)
MAY 79 A J DURELLI, K RAJAIAH N00014-76-C-0487
UNCLASSIFIED 51 NL

1 OF 1
AD A068265

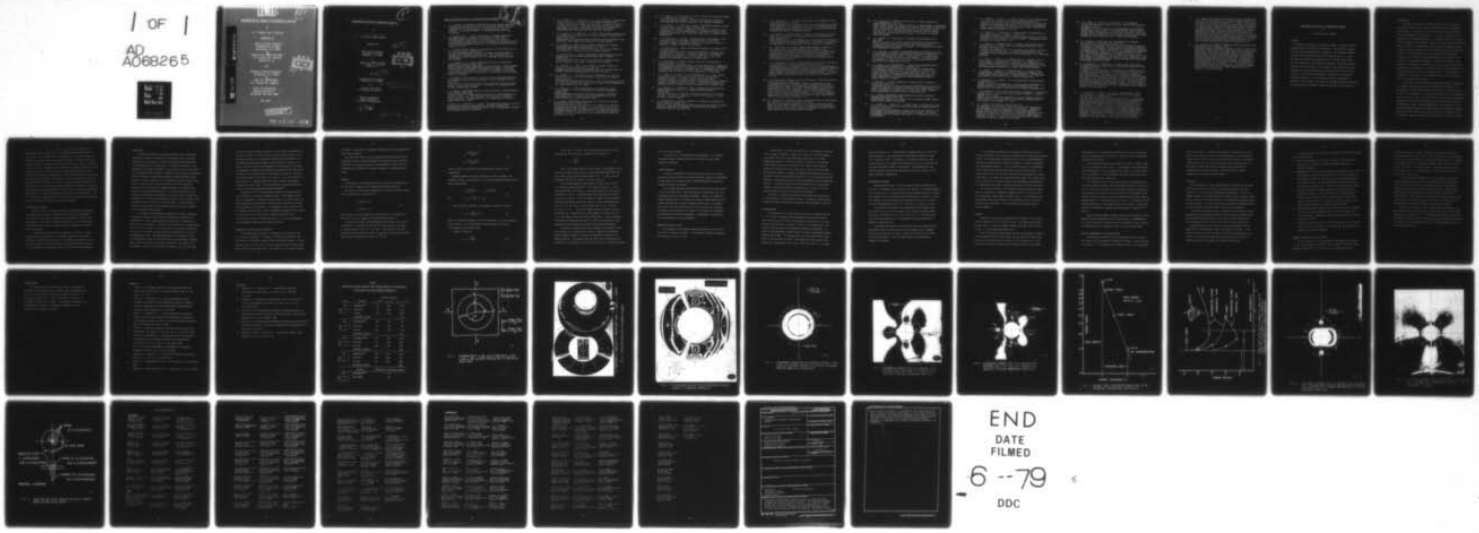

END
DATE FILMED
6 -79
DDC

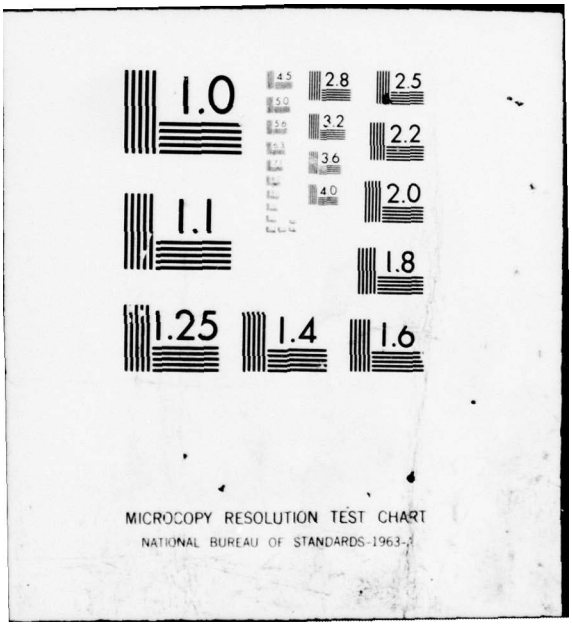
1.0
1.1
1.25
1.4
1.6
1.8
2.0
2.2
2.5
2.8
3.2
3.6
4.0
4.5
5.0
5.6
6.3
7.1
8.0
9.0
MICROCOPY RESOLUTION TEST CHART
NATIONAL BUREAU OF STANDARDS-1963-A

DETERMINATION OF STRAINS IN PHOTOELASTIC COATINGS

BY

A. J. DURELLI AND K. RAJAIAH

SPONSORED BY

OFFICE OF NAVAL RESEARCH
DEPARTMENT OF THE NAVY
WASHINGTON, D.C. 20025
ON
CONTRACT No. N0014-76-C-0487
O.U. PROJECT No. 31414-24
REPORT No. 51

AND

NATIONAL SCIENCE FOUNDATION
WASHINGTON, D.C. 20550
ON
GRANT No. ENG77-07974
O.U. PROJECT No. 32110-18

SCHOOL OF ENGINEERING
OAKLAND UNIVERSITY
ROCHESTER, MICHIGAN 48063

MAY 1979

(1)

(6) DETERMINATION OF STRAINS IN PHOTOELASTIC COATINGS

by

(10) A. J. Durelli and K. Rajaiah

Sponsored by

(12) 48p.

Office of Naval Research
Department of the Navy
Washington, D.C. 20025

on

Contract No. N0014-76-C-0487
O.U. Project No. 31313-24
Report No. 51

and (14) 51

National Science Foundation
Washington, D.C. 20550

on

(15) NØØ14-76-C-Ø487
NSF-ENG77-Ø7974

Grant No. ENG77-07974
O.U. Project No. 32110-18

School of Engineering
Oakland University
Rochester, Michigan 48063

(11) May 1979

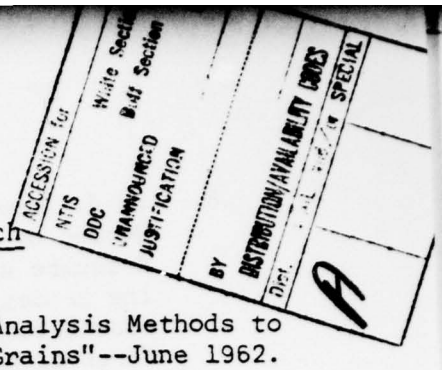

Previous Technical Reports to the Office of Naval Research

1. A. J. Durelli, "Development of Experimental Stress Analysis Methods to Determine Stresses and Strains in Solid Propellant Grains"--June 1962.
Developments in the manufacturing of grain-propellant models are reported. Two methods are given: a) cementing routed layers and b) casting.

2. A. J. Durelli and V. J. Parks, "New Method to Determine Restrained Shrinkage Stresses in Propellant Grain Models"--October 1962.
The birefringence exhibited in the curing process of a partially restrained polyurethane rubber is used to determine the stress associated with restrained shrinkage in models of solid propellant grains partially bonded to the case.

3. A. J. Durelli, "Recent Advances in the Application of Photoelasticity in the Missile Industry"--October 1962.
Two- and three-dimensional photoelastic analysis of grains loaded by pressure and by temperature are presented. Some applications to the optimization of fillet contours and to the redesign of case joints are also included.

4. A. J. Durelli and V. J. Parks, "Experimental Solution of Some Mixed Boundary Value Problems"--April 1964.
Means of applying known displacements and known stresses to the boundaries of models used in experimental stress analysis are given. The application of some of these methods to the analysis of stresses in the field of solid propellant grains is illustrated. The presence of the "pinching effect" is discussed.

5. A. J. Durelli, "Brief Review of the State of the Art and Expected Advance in Experimental Stress and Strain Analysis of Solid Propellant Grains"--April 1964.
A brief review is made of the state of the experimental stress and strain analysis of solid propellant grains. A discussion of the prospects for the next fifteen years is added.

6. A. J. Durelli, "Experimental Strain and Stress Analysis of Solid Propellant Rocket Motors"--March 1965.
A review is made of the experimental methods used to strain-analyze solid propellant rocket motor shells and grains when subjected to different loading conditions. Methods directed at the determination of strains in actual rockets are included.

7. L. Ferrer, V. J. Parks and A. J. Durelli, "An Experimental Method to Analyze Gravitational Stresses in Two-Dimensional Problems"--October 1965.
Photoelasticity and moiré methods are used to solve two-dimensional problems in which gravity-stresses are present.

8. A. J. Durelli, V. J. Parks and C. J. del Rio, "Stresses in a Square Slab Bonded on One Face to a Rigid Plate and Shrunk"--November 1965.
A square epoxy slab was bonded to a rigid plate on one of its faces in the process of curing. In the same process the photoelastic effects associated with a state of restrained shrinkage were "frozen-in." Three-dimensional photoelasticity was used in the analysis.

9. A. J. Durelli, V. J. Parks and C. J. del Rio, "Experimental Determination of Stresses and Displacements in Thick-Wall Cylinders of Complicated Shape"--April 1966.
Photoelasticity and moiré are used to analyze a three-dimensional rocket shape with a star shaped core subjected to internal pressure.

10. V. J. Parks, A. J. Durelli and L. Ferrer, "Gravitational Stresses Determined Using Immersion Techniques"--July 1966.
The methods presented in Technical Report No. 7 above are extended to three-dimensions. Immersion is used to increase response.

11. A. J. Durelli and V. J. Parks, "Experimental Stress Analysis of Loaded Boundaries in Two-Dimensional Second Boundary Value Problems"--February 1967.
The pinching effect that occurs in two-dimensional bonding problems, noted in Reports 2 and 4 above, is analyzed in some detail.

12. A. J. Durelli, V. J. Parks, H. C. Feng and F. Chiang, "Strains and Stresses in Matrices with Inserts,"-- May 1967.
Stresses and strains along the interfaces, and near the fiber ends, for different fiber end configurations, are studied in detail.

13. A. J. Durelli, V. J. Parks and S. Uribe, "Optimization of a Slot End Configuration in a Finite Plate Subjected to Uniformly Distributed Load,"--June 1967.
Two-dimensional photoelasticity was used to study various elliptical ends to a slot, and determine which would give the lowest stress concentration for a load normal to the slot length.

14. A. J. Durelli, V. J. Parks and Han-Chow Lee, "Stresses in a Split Cylinder Bonded to a Case and Subjected to Restrained Shrinkage,"--January 1968.
A three-dimensional photoelastic study that describes a method and shows results for the stresses on the free boundaries and at the bonded interface of a solid propellant rocket.

15. A. J. Durelli, "Experimental Stress Analysis Activities in Selected European Laboratories"--August 1968.
This report has been written following a trip conducted by the author through several European countries. A list is given of many of the laboratories doing important experimental stress analysis work and of the people interested in this kind of work. An attempt has been made to abstract the main characteristics of the methods used in some of the countries visited.

16. V. J. Parks, A. J. Durelli and L. Ferrer, "Constant Acceleration Stresses in a Composite Body"--October 1968.
Use of the immersion analogy to determine gravitational stresses in two-dimensional bodies made of materials with different properties.

17. A. J. Durelli, J. A. Clark and A. Kochev, "Experimental Analysis of High Frequency Stress Waves in a Ring"--October 1968.
A method for the complete experimental determination of dynamic stress distributions in a ring is demonstrated. Photoelastic data is supplemented by measurements with a capacitance gage used as a dynamic lateral extensometer.

18. J. A. Clark and A. J. Durelli, "A Modified Method of Holographic Interferometry for Static and Dynamic Photoelasticity"--April 1968.
A simplified absolute retardation approach to photoelastic analysis is described. Dynamic isopachics are presented.

19. J. A. Clark and A. J. Durelli, "Photoelastic Analysis of Flexural Waves in a Bar"--May 1969.
A complete direct, full-field optical determination of dynamic stress distribution is illustrated. The method is applied to the study of flexural waves propagating in a urethane rubber bar. Results are compared with approximate theories of flexural waves.

20. J. A. Clark and A. J. Durelli, "Optical Analysis of Vibrations in Continuous Media"--June 1969.
Optical methods of vibration analysis are described which are independent of assumptions associated with theories of wave propagation. Methods are illustrated with studies of transverse waves in prestressed bars, snap loading of bars and motion of a fluid surrounding a vibrating bar.

21. V. J. Parks, A. J. Durelli, K. Chandrashekhara and T. L. Chen, "Stress Distribution Around a Circular Bar, with Flat and Spherical Ends, Embedded in a Matrix in a Triaxial Stress Field"--July 1969.
A Three-dimensional photoelastic method to determine stresses in composite materials is applied to this basic shape. The analyses of models with different loads are combined to obtain stresses for the triaxial cases.

22. A. J. Durelli, V. J. Parks and L. Ferrer, "Stresses in Solid and Hollow Spheres Subjected to Gravity or to Normal Surface Tractions"--October 1969.
The method described in Report No. 10 above is applied to two specific problems. An approach is suggested to extend the solutions to a class of surface traction problems.

23. J. A. Clark and A. J. Durelli, "Separation of Additive and Subtractive Moiré Patterns"--December 1969.
A spatial filtering technique for adding and subtracting images of several gratings is described and employed to determine the whole field of Cartesian shears and rigid rotations.

24. R. J. Sanford and A. J. Durelli, "Interpretation of Fringes in Stress-Holo-Interferometry"--July 1970.
Errors associated with interpreting stress-holo-interferometry patterns as the superposition of isopachics (with half order fringe shifts) and isochromatics are analyzed theoretically and illustrated with computer generated holographic interference patterns.

25. J. A. Clark, A. J. Durelli and P. A. Laura, "On the Effect of Initial Stress on the Propagation of Flexural Waves in Elastic Rectangular Bars"--December 1970.
Experimental analysis of the propagation of flexural waves in prismatic, elastic bars with and without prestressing. The effects of prestressing by axial tension, axial compression and pure bending are illustrated.

26. A. J. Durelli and J. A. Clark, "Experimental Analysis of Stresses in a Buoy-Cable System Using a Birefringent Fluid"--February 1971.
An extension of the method of photoviscous analysis is presented which permits quantitative studies of strains associated with steady state vibrations of immersed structures. The method is applied in an investigation of one form of behavior of buoy-cable systems loaded by the action of surface waves.

27. A. J. Durelli and T. L. Chen, "Displacements and Finite-Strain Fields in a Sphere Subjected to Large Deformations"--February 1972.
Displacements and strains (ranging from 0.001 to 0.50) are determined in a polyurethane sphere subjected to several levels of diametral compression. A 500 lines-per-inch grating was embedded in a meridian plane of the sphere and moiré effect produced with a non-deformed master. The maximum applied vertical displacement reduced the diameter of the sphere by 27 per cent.

28. A. J. Durelli and S. Machida, "Stresses and Strain in a Disk with Variable Modulus of Elasticity"--March 1972
A transparent material with variable modulus of elasticity has been manufactured that exhibits good photoelastic properties and can also be strain analyzed by moiré. The results obtained suggests that the stress distribution in the disk of variable E is practically the same as the stress distribution in the homogeneous disk. It also indicates that the strain fields in both cases are very different, but that it is possible, approximately, to obtain the stress field from the strain field using the value of E at every point, and Hooke's law.

29. A. J. Durelli and J. Buitrago, "State of Stress and Strain in a Rectangular Belt Pulled Over a Cylindrical Pulley"--June 1972.
Two- and three-dimensional photoelasticity as well as electrical strain gages, dial gages and micrometers are used to determine the stress distribution in a belt-pulley system. Contact and tangential stress for various contact angles and friction coefficients are given.

30. T. L. Chen and A. J. Durelli, "Stress Field in a Sphere Subjected to Large Deformations"--June 1972.
Strain fields obtained in a sphere subjected to large diametral compressions from a previous paper were converted into stress fields using two approaches. First, the concept of strain-energy function for an isotropic elastic body was used. Then the stress field was determined with the Hookean type natural stress-natural strain relation. The results so obtained were also compared.

31. A. J. Durelli, V. J. Parks and H. M. Hasseem, "Helices Under Load"--July 1973.
Previous solutions for the case of close coiled helical springs and for helices made of thin bars are extended. The complete solution is presented in graphs for the use of designers. The theoretical development is correlated with experiments.

32. T. L. Chen and A. J. Durelli, "Displacements and Finite Strain Fields in a Hollow Sphere Subjected to Large Elastic Deformations"--September 1973.
The same methods described in No. 27, were applied to a hollow sphere with an inner diameter one half the outer diameter. The hollow sphere was loaded up to a strain of 30 per cent on the meridian plane and a reduction of the diameter by 20 per cent.

33. A. J. Durelli, H. H. Hasseem and V. J. Parks, "New Experimental Method in Three-Dimensional Elastostatics"--December 1973.
A new material is reported which is unique among three-dimensional stress-freezing materials, in that, in its heated (or rubbery) state it has a Poisson's ratio which is appreciably lower than 0.5. For a loaded model, made of this material, the unique property allows the direct determination of stresses from strain measurements taken at interior points in the model.

34. J. Wolak and V. J. Parks, "Evaluation of Large Strains in Industrial Applications"--April 1974.
It was shown that Mohr's circle permits the transformation of strain from one axis of reference to another, irrespective of the magnitude of the strain, and leads to the evaluation of the principal strain components from the measurement of direct strain in three directions.

35. A. J. Durelli, "Experimental Stress Analysis Activities in Selected European Laboratories"--April 1975.
Continuation of Report No. 15 after a visit to Belgium, Holland, Germany, France, Turkey, England and Scotland.

36. A. J. Durelli, V. J. Parks and J. O. Bühler-Vidal, "Linear and Non-linear Elastic and Plastic Strains in a Plate with a Big Hole Loaded Axially in its Plane"--July 1975.
Strain analysis of the ligament of a plate with a big hole indicates that both geometric and material non-linearity may take place. The strain concentration factor was found to vary from 1 to 2 depending on the level of deformation.

37. A. J. Durelli, V. Pavlin, J. O. Bühler-Vidal and G. Ome, "Elastostatics of a Cubic Box Subjected to Concentrated Loads"--August 1975.
Analysis of experimental strain, stress and deflection of a cubic box subjected to concentrated loads applied at the center of two opposite faces. The ratio between the inside span and the wall thickness was varied between approximately 5 and 121.

38. A. J. Durelli, V. J. Parks and J. O. Bühler-Vidal, "Elastostatics of Cubic Boxes Subjected to Pressure"--March 1976.
Experimental analysis of strain, stress and deflections in a cubic box subjected to either internal or external pressure. Inside span-to-wall thickness ratio varied from 5 to 14.

39. Y. Y. Hung, J. D. Hovanesian and A. J. Durelli, "New Optical Method to Determine Vibration-Induced Strains with Variable Sensitivity After Recording"--November 1976.
A steady state vibrating object is illuminated with coherent light and its image slightly misfocused. The resulting specklegram is "time-integrated" as when Fourier filtered gives derivatives of the vibrational amplitude.

40. Y. Y. Hung, C. Y. Liang, J. D. Hovanesian and A. J. Durelli, "Cyclic Stress Studies by Time-Averaged Photoelasticity"--November 1976.
"Time-averaged isochromatics" are formed when the photographic film is exposed for more than one period. Fringes represent amplitudes of the oscillating stress according to the zeroth order Bessel function.

41. Y. Y. Hung, C. Y. Liang, J. D. Hovanesian and A. J. Durelli, "Time-Averaged Shadow Moiré Method for Studying Vibrations"--November 1976.
Time-averaged shadow moiré permits the determination of the amplitude distribution of the deflection of a steady vibrating plate.

42. J. Buitrago and A. J. Durelli, "On the Interpretation of Shadow-Moiré Fringes"--April 1977.
Possible rotations and translations of the grating are considered in a general expression to interpret shadow-moiré fringes and on the sensitivity of the method. Application to an inverted perforated tube.

43. J. der Hovanesian, "18th Polish Solid Mechanics Conference." Published in European Scientific Notes of the Office of Naval Research, in London, England, Dec. 31, 1976.
Comments on the planning and organization of, and scientific content of paper presented at the 18th Polish Solid Mechanics Conference held in Wisla-Jawornik from September 7-14, 1976.

44. A. J. Durelli, "The Difficult Choice,"--May 1977.
The advantages and limitations of methods available for the analyses of displacements, strain, and stresses are considered. Comments are made on several theoretical approaches, in particular approximate methods, and attention is concentrated on experimental methods: photo-elasticity, moiré, brittle and photoelastic coatings, gages, grids, holography and speckle to solve two- and three-dimensional problems in elasticity, plasticity, dynamics and anisotropy.

45. C. Y. Liang, Y. Y. Hung, A. J. Durelli and J. D. Hovanesian, "Direct Determination of Flexural Strains in Plates Using Projected Gratings,"--June 1977.
The method requires the rotation of one photograph of the deformed grating over a copy of itself. The moiré produced yields strains by optical double differentiation of deflections. Applied to projected gratings the idea permits the study of plates subjected to much larger deflections than the ones that can be studied with holograms.

46. A. J. Durelli, K. Brown and P. Yee, "Optimization of Geometric Discontinuities in Stress Fields"--March 1978.
The concept of "coefficient of efficiency" is introduced to evaluate the degree of optimization. An ideal design of the inside boundary of a tube subjected to diametral compression is developed which decreases its maximum stress by 25%, at the time it also decreases its weight by 10%. The efficiency coefficient is increased from 0.59 to 0.95. Tests with a brittle material show an increase in strength of 20%. An ideal design of the boundary of the hole in a plate subjected to axial load reduces the maximum stresses by 26% and increases the coefficient of efficiency from 0.54 to 0.90.

47. J. D. Hovanesian, Y. Y. Hung and A. J. Durelli, "New Optical Method to Determine Vibration-Induced Strains With Variable Sensitivity After Recording"--May 1978.
A steady-state vibrating object is illuminated with coherent light and its image is slightly misfocused in the film plane of a camera. The resulting processed film is called a "time-integrated specklegram." When the specklegram is Fourier filtered, it exhibits fringes depicting derivatives of the vibrational amplitude. The direction of the spatial derivative, as well as the fringe sensitivity may be easily and continuously varied during the Fourier filtering process. This new method is also much less demanding than holographic interferometry with respect to vibration isolation, optical set-up time, illuminating source coherence, required film resolution. etc.

48. Y. Y. Hung and A. J. Durelli, "Simultaneous Determination of Three Strain Components in Speckle Interferometry Using a Multiple Image Shearing Camera,"--September 1978
This paper describes a multiple image-shearing camera. Incorporating coherent light illumination, the camera serves as a multiple shearing speckle interferometer which measures the derivatives of surface displacements with respect to three directions simultaneously. The application of the camera to the study of flexural strains in bent plates is shown, and the determination of the complete state of two-dimensional strains is also considered. The multiple image-shearing camera uses an interference phenomena, but is less demanding than holographic interferometry with respect to vibration isolation and the coherence of the light source. It is superior to other speckle techniques in that the obtained fringes are of much better quality.

49. A. J. Durelli and K. Rajaiah, "Quasi-square Hole With Optimum Shape in an Infinite Plate Subjected to In-plane Loading"--January 1979. This paper deals with the optimization of the shape of the corners and sides of a square hole, located in a large plate and subjected to in-plane loads. Appreciable disagreement has been found between the results obtained previously by other investigators. Using an optimization technique, the authors have developed a quasi-square shape which introduces a stress concentration of only 2.54 in a uniaxial field, the comparable value for the circular hole being 3. The efficiency factor of the proposed optimum shape is 0.90. whereas the one of the best shape developed previously was 0.71. The shape also is developed that minimizes the stress concentration in the case of biaxial loading when the ratio of biaxiality is 1:-1.

50. A. J. Durelli and K. Rajaiah, "Optimum Hole Shapes in Finite Plates Under Uniaxial Load,"--February 1979.
This paper presents optimized hole shapes in plates of finite width subjected to uniaxial load for a large range of hole to plate widths (D/W) ratios. The stress concentration factor for the optimized holes decreased by as much as 44% when compared to circular holes. Simultaneously, the area covered by the optimized hole increased by as much as 26% compared to the circular hole. Coefficients of efficiency between 0.91 and 0.96 are achieved. The geometries of the optimized holes for the D/W ratios considered are presented in a form suitable for use by designers. It is also suggested that the developed geometries may be applicable to cases of rectangular holes and to the tip of a crack. This information may be of interest in fracture mechanics.

DETERMINATION OF STRAINS IN PHOTOELASTIC COATINGS

by

A. J. Durelli and K. Rajaiah

ABSTRACT

Photoelastic coatings can be cemented directly to actual structural components and tested under field conditions. This important advantage has made them relatively popular in industry. The information obtained, however, may be misinterpreted and lead to serious errors. A correct interpretation requires the separation of the principal strains and so far, this operation has been found very difficult. Following a previous paper by one of the authors, it is proposed to drill small holes in the coating and record the birefringence at points removed from the edge of the holes. The theoretical background of the method is reviewed; the technique necessary to use it is explained and two applications are described. The precision of the method is evaluated and found satisfactory in contradiction to information previously published in the literature.

INTRODUCTION

Covering the surfaces of engineering structures with transparent coatings and recording the changes in birefringence with a reflection polariscrope, is the basis of a method that can find many applications. The main advantages of the method are: 1) no model is required, 2) the knowledge of the loading conditions is not necessary either, and 3) whole-field information can be obtained. Besides the usual technical difficulties that are common to all experimental methods (accurate machining, proper cementing, correct recording, etc.) the method has some very serious limitations. The first one of these limitations is the low sensitivity associated with relatively thin coatings cemented to the commonly used relatively rigid engineering materials. The second limitation is that, although the information is available for the whole field, in general the evaluation has to be done point-by-point not only for the directions of the principal stresses but also for the maximum shear. A third important limitation is the nature of the information that can be easily obtained, as to be explained in what follows.

In the classic two-dimensional photoelasticity analysis, separation of stresses is seldom required since most analyses are directed to the determination of stress concentrations and these occur in plates most of the time at free boundaries. This means that actually only a unidimensional state of stress is solved. On the other hand, the surfaces of engineering structures to be covered with coatings can be considered as in a state of two-dimensional stress. The main implication of this situation is that the maximum shears present at the surfaces are not necessarily the maximum shears in the body, which are the ones of interest to the analyst and to the designer. Wherever the two principal stresses σ_1 and σ_2 in the plane

of the surface are of the same sign, $(\sigma_1 - \sigma_2)/2$ does not represent the maximum shear stress at that point. The maximum principal shear stress is $\sigma_1/2$ or $\sigma_2/2$. The statement can be illustrated by also calling attention to points of zero fringe order in photoelastic coatings. At these points, both principal stresses are equal but both could have very large values. Therefore, a point, or a zone, of apparently low stress may be actually subjected to a very high shear on a plane off the coating. To bypass this difficulty, several attempts have been made at separating the two principal stresses that take place in the plane of the coating. This has been so far a very difficult task whatever the method to be used. In this paper, a method proposed by Tesar[1] and modified by one of the authors many years ago[2] will be developed to transform the coating into a situation similar to the one found in classic two-dimensional photoelasticity for which the determinations are made at free boundaries. The "strip" method is a similar method that has also been proposed, and a comparison of the two methods will be made at the end of the paper.

PRINCIPLE OF THE METHOD

Instead of using a continuous coating, the coating will be perforated with small circular holes of a diameter of the order of the thickness of the coating and at a distance from each other sufficiently large to avoid interference. This artifice creates free boundaries in the coating and at these boundaries the stress is uniaxial and can be completely determined in a direct manner.

In the previous publication[2], an analysis of the state of stress around an empty circular hole in a thin plate subjected to any biaxial condition of stress has been presented. The problem was completely solved, the results shown in tabulated form and the following conclusions reached: 1) the direction of the principal stress in the structure can be obtained

INTRODUCTION

Covering the surfaces of engineering structures with transparent coatings and recording the changes in birefringence with a reflection polariscrope, is the basis of a method that can find many applications. The main advantages of the method are: 1) no model is required, 2) the knowledge of the loading conditions is not necessary either, and 3) whole-field information can be obtained. Besides the usual technical difficulties that are common to all experimental methods (accurate machining, proper cementing, correct recording, etc.) the method has some very serious limitations. The first one of these limitations is the low sensitivity associated with relatively thin coatings cemented to the commonly used relatively rigid engineering materials. The second limitation is that, although the information is available for the whole field, in general the evaluation has to be done point-by-point not only for the directions of the principal stresses but also for the maximum shear. A third important limitation is the nature of the information that can be easily obtained, as to be explained in what follows.

In the classic two-dimensional photoelasticity analysis, separation of stresses is seldom required since most analyses are directed to the determination of stress concentrations and these occur in plates most of the time at free boundaries. This means that actually only a unidimensional state of stress is solved. On the other hand, the surfaces of engineering structures to be covered with coatings can be considered as in a state of two-dimensional stress. The main implication of this situation is that the maximum shears present at the surfaces are not necessarily the maximum shears in the body, which are the ones of interest to the analyst and to the designer. Wherever the two principal stresses σ_1 and σ_2 in the plane

without the need of recording isoclinics in the coating by recording only the axes of symmetry of the isochromatic pattern around the hole; 2) the principal stresses can be determined by addition and subtraction of the factored maximum and minimum values of the isochromatic fringes at the edge of the hole; and 3) since frequently the fringe orders at the edges of photoelastic materials are determined less precisely than those inside the field, it was proposed that the measurements be taken at a distance from the edge equal to the radius of the hole ($r = 2a$), rather than at the edge of the hole. Equations have been given to compute the principal stresses using these values. The above method has also been applied successfully to certain restrained shrinkage problems[3].

Nisida et al [4][5] had considered the small hole drilling method in the context of determining residual stresses. Their approach, which uses only photoelastic information from the edges of the holes, shows such large differences from theoretical values that the conclusion is reached that the method is not applicable. The assumption is that near the hole a "thickness effect" does not permit a meaningful evaluation of the strains. The work reported here shows that much smaller differences occur. It also shows that when the values are taken at $r = 2a$, the determination of the principal strains can be sufficiently precise.

ADVANTAGES AND LIMITATIONS OF THE METHOD

The proposed method increases the response of the coating by from 2 to 4 orders of magnitude. It permits the direct determination of the directions of the principal stresses without recording isoclinics. It gives individual values of each of the principal stresses directly without supplementary tests or major computations. The precision of the results obtained

is higher. In many cases, photographic recording and use of monochromatic light will be possible.

The method will require that the coating be perforated either before cementing or after it has been cemented to the surface of the structure. Errors may be introduced in zones of high gradients of stress since the formulae used to interpret the results correspond to a uniform state of stress.

ANALYSIS

The direction of the principal stresses is given by the direction of the two axes of symmetry of the fringe pattern around each hole.

The values of the principal stresses at the center of the hole, before the hole was drilled, are given by[2]:

$$\sigma_1 = \frac{1}{8}(\sigma_A + 3\sigma_B)$$
$$\sigma_2 = \frac{1}{8}(3\sigma_A + \sigma_B) \qquad (1)$$

where σ_A and σ_B are the stresses at the intersection of the edge of the hole with the axes of symmetry of the fringe pattern (Fig. 1).

To be more practical, the measurements can be taken on the two axes of symmetry at a distance from the edge of the hole equal to the radius of the hole (points C and E on r = 2a line). The equations to be used, developed from the general equations of isochromatics in any biaxial stress field around a circular hole, as given in [2] are:

$$\sigma_1 = \frac{(15\sigma_E + 7\sigma_C)}{11}$$

$$\sigma_2 = \frac{(15\sigma_C + 7\sigma_E)}{11} \qquad (2)$$

where σ_C and σ_E are principal stress differences at points C and E respectively.

Coatings analyses are usually conducted in terms of strains. The principal strains ε_1 and ε_2 and $(\varepsilon_1 - \varepsilon_2)$ can be determined from the stress-strain relationships

$$\varepsilon_1 = \frac{\sigma_1 - \nu\sigma_2}{E} \quad ; \quad \varepsilon_2 = \frac{\sigma_2 - \nu\sigma_1}{E} \qquad (3)$$

and $$\varepsilon_1 - \varepsilon_2 = \frac{1 + \nu}{E} (\sigma_1 - \sigma_2)$$

The strain optic relation for photoelastic coatings is given by

$$\varepsilon_1 - \varepsilon_2 = \frac{\lambda n}{2t_c K} = nf_\varepsilon \qquad (4)$$

where K is a material constant, n is the fringe order, t_c is the thickness of the coating, λ is the wavelength of light used and $f_\varepsilon (= \lambda/2t_c K)$ is the material strain fringe value.

From Eqs. (3) and (4)

$$\sigma_1 - \sigma_2 = \frac{f_\varepsilon E}{1+\nu} n \qquad (5)$$

On the edge of the hole, one of the principal stresses is zero; then from Eq. (5) the stress σ_t tangential to the hole is:

$$\sigma_t = \frac{f_\varepsilon E}{1+\nu} n \qquad (6)$$

Thus, if the fringe orders at the two points of intersection of the two axes of symmetry with the hole edge are determined along with their sign, then σ_A and σ_B can be obtained from Eq. (6). σ_1 and σ_2 are then calculated from Eq. (1), and Eq. (3) gives ε_1 and ε_2.

In the second approach, fringe orders at points C and E on the r = 2a line are determined and Eq. (5) is used to obtain $(\sigma_1 - \sigma_2)$ at those points, which are σ_C and σ_E. Using these values, Eq. (2) is used to determine σ_1 and σ_2. Sometimes doubts may exist about the signs to be given to σ_C and σ_E. It may be helpful to remember that the signs of these stresses are the same as the signs of σ_A and σ_B respectively for all $\sigma_1/\sigma_2 < 0$. For $\sigma_1/\sigma_2 > 0$ in the ranges $7/15 > \sigma_1/\sigma_2 > 1/3$ and $3 > \sigma_1/\sigma_2 > 15/7$, σ_C has the opposite sign of σ_A while σ_E has the same sign as σ_B. Outside these two short ranges, the signs of σ_C and σ_E are the same as those of σ_A and σ_B respectively. It may be practical to determine the magnitude and sign of σ_1 and σ_2 first using the first approach, and then improve the precision using the second approach.

Invariably, residual stresses may be expected to be present around the hole edges due to absorption or release of moisture, differential thermal expansion between the coating and the model, shrinkage of the adhesive bond etc. The magnitude and the sign of this stress have to be evaluated at the beginning of the test and they have to be properly accounted

for in the final analysis.

The method will be illustrated with two examples: 1) a circular disk under diametral compression and 2) a circular ring also under diametral compression.

COATING MATERIALS

The basic requirements of the method are the choice of a coating material with high sensitivity and good reflective properties, introduction of small holes in the coating without creating machining stresses and a suitable reflection polariscope.

Of the common materials, polycarbonates seem the best suited because of their high sensitivity. Materials supplied by Photoelastic Inc. were used because they were conveniently available. However, the reflective coating supplied with "PS-1" appears very coarse on magnification and the fringes are difficult to identify around the small holes. The epoxies "PS-2" and "PS-8" were chosen and one of their surfaces was coated with an aluminium undercoating and then bonded to the model with an adhesive. This provided good reflective background. Unfortunately, these epoxies are less sensitive than the polycarbonate.

INTRODUCTION OF SMALL HOLES

The thickness of the suitable coating varies usually from 0.07 in. to 0.125 in. (1.78 mm to 3.18 mm). It was decided to choose the diameter of the holes as 0.1 in. (2.5 mm).

The machining of the hole was carried out in five stages of drilling and two stages of reaming. A pilot hole of 0.031 in. (0.79 mm) diameter was drilled first and it was progressively increased till the final diameter was reached. In order to minimize the effect of the residual stresses which may have been produced by the cement at the interface between the coating and the body, and also (in case the holes have been drilled before bonding) to prevent the adhesive from getting into the hole, the depth of the hole was stopped at about 0.01 in. (0.25 mm) away from the interface. These precautions lead to holes practically free from machining stresses. If residual stresses have been produced by other causes like exchange of moisture, variation in temperature, etc., they will show as fringes around the holes and they have to be determined.

The edge of the holes were covered with non-reflective black paint to avoid reflection and scattering of light. A drawback of this procedure is that both light and dark fields appear with dark background in the hole.

THE POLARISCOPE

As a consequence of the fact that the holes to be observed have only 0.1 in. (2.5 mm) in diameter, the polariscope to be used should have a high resolution power and give, with precision, the details of the fringe pattern around the edges. Incidence of light is not perpendicular to the surface of the coating in the conventional reflection polariscopes. It cannot be used among other reasons because it produces unacceptable shadows around the hole edges. A new polariscope with a ring shaped light source, similar to the one used by Slot[6], was designed and built around a ring shaped Aristo monochromatic light source of 100 watts (Fig. 2). The light

source has about 5.5 in. (140 mm) external diameter and 1.75 in. (44.5 mm) internal diameter. With this smaller central opening compared to about 4 in. (100 mm) of Slot's polariscope, it is possible to keep the light source very close to the model (at a distance of say 12 in.) and still have the light practically normal to the surface. The polariscope has both plane and circular polarization capability as well as the ability to use Tardy's method of compensation.

EXPERIMENTAL PROCEDURE

Epoxy plates 0.625 in. (15.9 mm) thick were chosen to make the ring and disk. The diameter of the disk was 4 in. (102 mm). The internal diameter of the ring was 4.5 in. (114 mm) and the external diameter was 9 in. (228 mm). The coating on the disk was made of epoxy (PS-8) with t = 0.072 in. (1.8 mm). The coatings on the ring were made of both epoxy (PS-2) with t = 0.082 in. (2.1 mm) and polycarbonate (PS-1) (K = 0.16) with t = 0.125 in. (3.2 mm).

The coatings were bonded to the specimens and after proper curing, small holes of 0.1 in. (2.5 mm) diameter were drilled as mentioned above, at points at distances of 0.5 in. (12.7 mm) or 0.75 in. (19 mm) from each other, and along radial lines. The specimens were then subjected to a diametral compressive load.

The coating materials on the ring and the disk were calibrated with measurements taken at several points on the horizontal axis of symmetry using the known theoretical values. K values of 0.132 for PS-2 and 0.089 for PS-8 were obtained. E for the model material was determined as 480,000 Psi (3310 MPa).

The birefringent response of the coating to residual as well as to stresses associated with the loads was studied using the polariscope described earlier. The fringe pattern around each of the holes was photographically recorded and enlarged about 15 times for analysis. Fringes are sometimes only approximately symmetric. The two axes were marked on the photograph and the fringe order distributions along the two axes were plotted. The fringe orders at the hole edge were determined by extrapolating the curves, and average of the values were obtained from both sides. The fringe values at $r = 2a$ along the two axes of symmetry were determined from the graph or by compensation using Tardy's method and the device to be described later.

The circular ring with the two types of coating perforated by small holes was subjected to a diametral compressive load of 714 lb. (3.24 kN). The corresponding fringe pattern is shown in Fig. 3. The response of the polycarbonate coating was higher; but the analysis could not be carried out due to poor resolution. Only information from the epoxy coating could be analyzed.

EXAMPLES

Consider the hole on the horizontal axis of symmetry ($\Theta = 0$) of the ring at a distance $r/b = 0.61$ from the center. The fringe pattern around the hole under no load (only residual stresses) and under load are shown in Figs. 4, 5 and 6 magnified several times.

Since the residual stresses around the hole are essentially isotropic with an exponential decay from the edge, the log-log plot of fringe order versus the radial distance from the edge will be a straight line. This plot gives an accurate estimation of the residual stresses at any radial

distance (Fig. 7). The sign of the residual stress can be obtained by using some compensators or by applying a load to the ring and observing the motion of the fringe.

The fringe order distributions along the two axes of symmetry when the ring is loaded are given in Fig. 8. The average of the distributions along the horizontal axis of symmetry on both sides of the hole is used for the calculations. The distributions along the vertical axis on the upper and lower sides are symmetrical.

The principal strains at the selected points are determined using the fringe order at the edge of the hole obtained from Fig. 8, and Eqs. (1) and (3). Since the hole does not go all the way through the coating, in the computations the depth of the hole was taken as the thickness of the coating. Principal strains are also determined using the fringe order at points located at r = 2a and using Eqs. (2) and (3). The residual strains obtained previously are subtracted from the total strains. The two sets of values so obtained are compared with those given by Timoshenko[7] in Table 1.

Using the same procedure, principal strains were determined at other points in both a circular disk and the circular ring. Illustrations of the patterns obtained for two other holes are presented in Figs. 9 and 10. The compared values are included in Table 1 for some typical points.

DEVICE TO COMPENSATE AT THE DESIRED POINTS

When the strain level is low, the determination on the 2a line of the value of the birefringence by compensation requires a precise location of the points. It was observed that scribing of lines on the coating may

distort the fringes. A simple circular device, as shown in Fig. 11, was used to increase the precision of the determinations. With this device plugged into the hole in the coating and each pair of holes in the device aligned with each of the two axes of symmetry of the fringe pattern, it was simple to locate the points and determine the fringe orders by compensation with greater precision. Since the device is opaque, extinction can be observed in high contrast.

DISCUSSION

The fringe pattern in Fig. 3 shows that the introduction of the small holes does not disturb the overall fringe pattern and their effect is confined to a small region in the immediate neighbourhood. The axes of symmetry around the holes determines the direction of the principal stresses without the need of recording isoclinics. The isochromatic patterns around the holes in Figs. 4 to 10 show that there is sufficient information around the holes from dark and bright fields to carry out the analysis.

The results presented in Table 1 indicate that the principal strains determined from fringe values obtained at the hole edge are somewhat lower than those obtained theoretically or by using other experimental means. The information from the 2a line is very close to those other values.

As already mentioned, the results for the disk were obtained at the beginning of the investigation using a less sensitive material. As the coating was applied to only one side of the disk, some bending effect was present. The results are found to deviate from the theoretical ones slightly more than the ones given in the Table for the ring.

The following points should, however, be borne in mind while commenting on the values presented.

a) Some of the measurements were taken at points at which the strain gradients were very high, to evaluate the method under less favorable conditions.

b) Measurements were all made in the presence of residual stresses. This also increases the difficulties since any error in the estimation of the residual stresses will lead to an error in the determination of the principal strains. The use of polycarbonate coatings with the proper reflecting surface will increase the precision in this respect.

c) The method of using information taken from the 2a line leads to satisfactory results. A closer analysis of the original paper[2] indicates that it would be better to take inside the field information at points located at a distance 1.4a from the center, rather than at points located at a distance 2a from the center.

d) Additional information along the two axes of symmetry can be obtained by the use of contour-equidensity film. This should improve the precision further. Reference to the use of this method can be found, for instance in[10].

e) The maximum strains taking place in the specimen used in this investigation, is of the same order as the strains that can be expected in engineering structural components.

COMMENTS ON THE HOLE AND STRIP METHODS

An idea, similar to the one developed in this paper was introduced at about the same time by O'Regan[11] and by Moench[12] and later further developed by Galster[13]. It consists in the transformation of the

continuous coating in a series of parallel strips separated by slots of about the same width as the strips. This method yields ε_y in the direction of the strip over the field, in a discontinuous manner along x. A variation of the method consists in having the separation between strips to operate also as a coating, but of smaller height. This lower coating would give the information $(\varepsilon_1 - \varepsilon_2)$ corresponding to a continuous coating, and the higher strips would give ε_y.

It is much easier to determine the axis of symmetry of the fringe pattern around the hole than the isoclinic fringes in the discontinuous strip field and the direction of the principal strains can therefore be determined with higher precision using the hole method. Since the strip method requires the knowledge of the isoclinic angle to determine the second principal strain, whereas the strains are determined directly using the hole method, the precision of the hole method is also higher for the determination of the individual values of the principal strains.

There are limitations to the use of photoelastic coatings when the state of stress in the material under it changes with time. Some of these limitations are reviewed in[14]. But whereas the disturbance introduced by the presence of strips in the field makes impossible any dynamic application, it is felt that the hole method can be used to determine strains in many quasi-static applications.

ACKNOWLEDGMENTS

The research program from which this paper was developed was supported by the National Science Foundation (Grant ENG-76-07974) and the Office of Naval Research (Contract No. N00014-76-C-0487). The authors are grateful to C. C. Astill of NSF and N. Perrone and N. Basdekas of ONR for their support. The manuscript reproduction has been prepared by P. Baxter. S. Nygren was responsible for the building of the reflection polariscope.

REFERENCES

1. Tesar V., "La Photoelasticimetrie et ses Applications dans les Constructions Aeronautiques", La Science Aerienne, Paris, p. 372, Sept. - Oct. 1932.

2. Durelli A. J. and Murray W. M., "Stress Distribution Around a Circular Discontinuity in Any Two-Dimensional System of Combined Stress", Proceedings of 14th Semi-Annual Eastern Photoelasticity Conference, Yale University, pp. 21-36, 1941.

3. Parks V. J. and Durelli A. J., "Stress Distribution at Variously Shaped Corners in Plates, Bonded on Two Long Edges, and Subjected to Restrained Shrinkage", Bulletin of Chemical Propulsion Information Agency, Publication No. 119, Oct. 1966.

4. Nisida M., "A Method for Measuring Stresses on Metal Surface Photoelastically", Sci. Papers I.P.C.R., Vol. 59, No. 2, pp. 69-77, 1965.

5. Nisida M. and Takabayashi H., "Thickness Effects in "Hole Method" and Applications of the Method to Residual Stress Measurement", Sci. Papers I.P.C.R., Vol. 59, No. 2, pp. 78-86, 1965.

6. Slot T., "Reflection Polariscope for Photography of Photoelastic Coatings", Exp. Mech., Vol. 3, pp. 41-47, 1963.

7. Timoshenko S. and Goodier J. N., "Theory of Elasticity", McGraw Hill Book Co., N.Y., 2nd. ed., pp. 121-122, 1951.

8. Frocht M. M., "Photoelasticity", Vol. II, John Wiley, N.Y., pp. 194-195, 1948.

9. Frocht M. M., "Photoelasticity", Vol. I, John Wiley, N.Y., p. 175, 1948.

References

10. Mehrotra, C. L. and Meyer, M. L., "Equidensometry Applied to Photoelasticity", Exp. Mech., Vol. 16, No. 10, pp. 383-388, Oct. 1976.

11. O'Reagan, R., "New Method for Determining Strains on the Surface of a Body with Photoelastic Coatings", Exp. Mech., Vol. 5, No. 8, pp. 241-246, 1965.

12. Moench, E., "Die Vollstaendige Bestimmung des Dehnungszustandes auf Oberflaechen durch photo-elastische Streifenschichten", Schweizerische Bauzeitung, Vol. 48, pp. 840-842, 1966.

13. Galster, D., Spannungsoptische Bestimmung von Dehnungen mit profilierten Oberflaechenschichten. Beitraege zur Spannungs und Dehnungsanalyse IV., Berlin, pp. 47-92, 1967.

14. Zandman, F., Redner S. and Dally J., "Photoelastic Coatings", SESA Monograph, No. 3, pp. 108-109, 1977.

TABLE 1

COMPARISON OF STRAINS OBTAINED USING SEVERAL METHODS ON A CIRCULAR RING AND CIRCULAR DISK UNDER DIAMETRAL COMPRESSION

POINT	SOLUTION	PRINCIPAL STRAINS $\varepsilon_1 \times 10^6$	$\varepsilon_2 \times 10^6$	$(\varepsilon_1 - \varepsilon_2)\ 10^6$
RING	THEORETICAL[7]	213	-1325	1538
$\frac{r}{b} = 0.61$	HOLE EDGE	75	-1083	1158
$\theta = 0^o$	2a LINE	256	-1392	1648
	CONTINUOUS COATING	-	-	1513
RING	THEORETICAL[7]	196	-215	411
$\frac{r}{b} = 0.83$	HOLE EDGE	151	-267	418
$\theta = 0^o$	2a LINE	187	-241	428
	CONTINUOUS COATING	-	-	394
RING	EXPERIMENTAL[8]	481	-982	1463
$\frac{r}{b} = 0.61$	HOLE EDGE	114	-998	1112
$\theta = 45^o$	2a LINE	600	-1032	1631
	CONTINUOUS COATING	-	-	1544
DISK	THEORETICAL[7]	824	-1347	2171
$\frac{r}{b} = 0$	HOLE EDGE	692	-1059	1751
$\theta = 90^o$	2a LINE	625	-1282	1907
	CONTINUOUS COATING	-	-	2069

	SOLUTION	INCLINATION OF PRINCIPAL STRAINS
RING	EXPERIMENTAL[9]	71^o
$\frac{r}{b} = 0.61$	HOLE METHOD	69^o
$\theta = 45^o$		

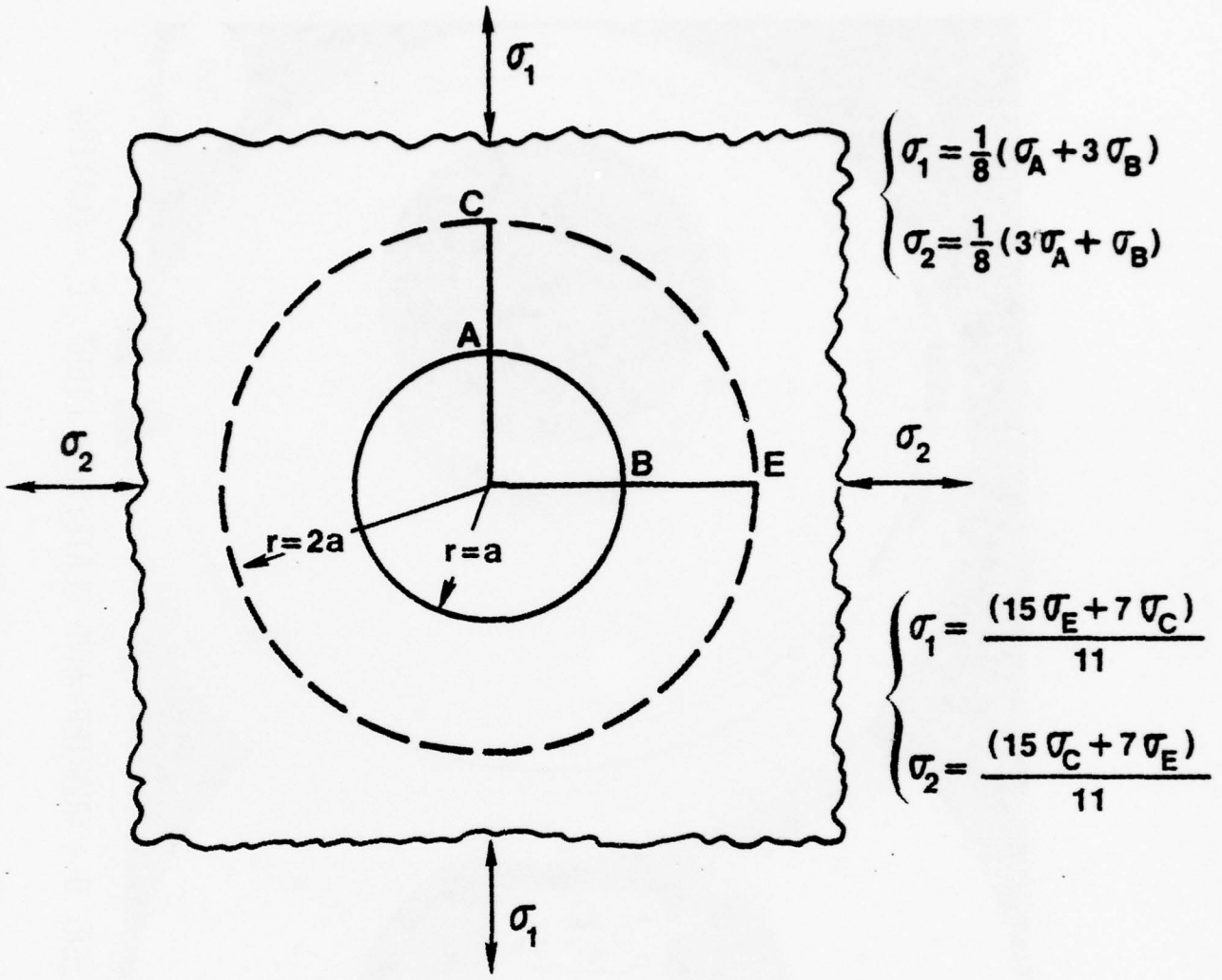

FIG. 1 DETERMINATION OF σ_1 AND σ_2 AS A FUNCTION OF σ_A AND σ_B AND σ_C AND σ_E USING A CIRCULAR HOLE IN THE BIAXIAL STRESS FIELD

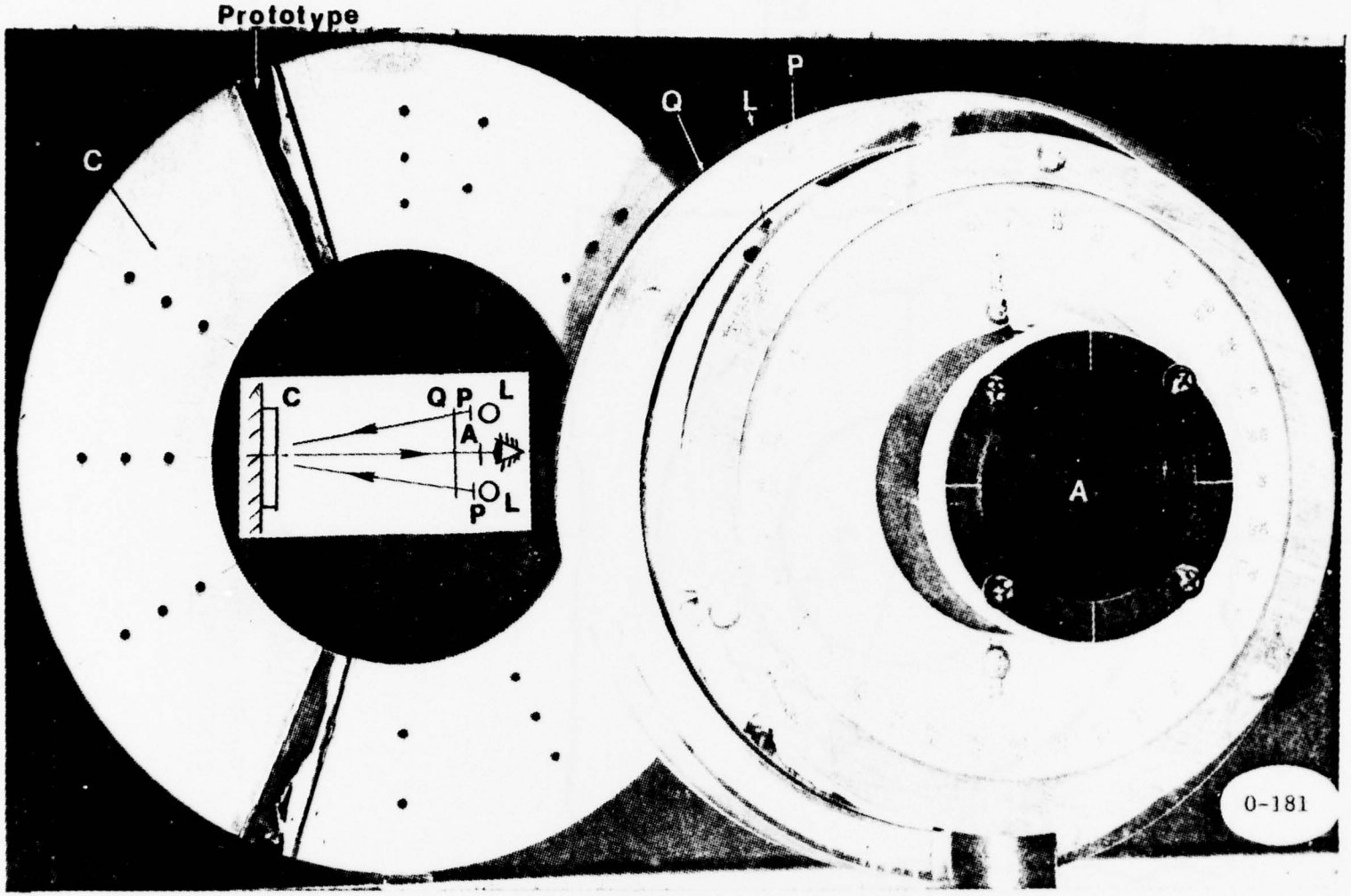

P = POLARIZER; A = ANALYZER; Q = QUARTER-WAVE PLATE; L = LIGHT; C = COATING

FIG. 2 REFLECTION POLARISCOPE FOR NORMAL INCIDENCE

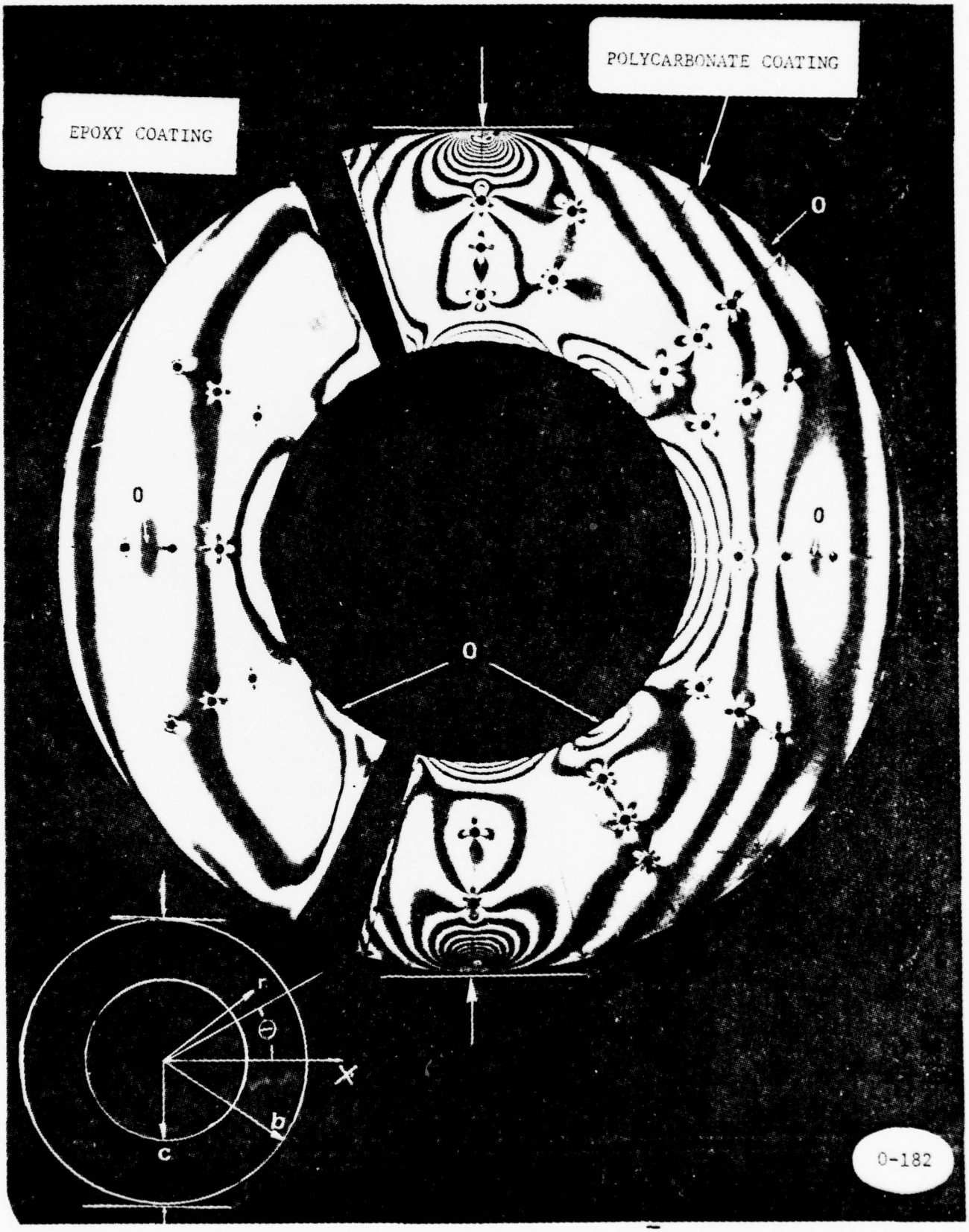

FIG. 3 CIRCULAR RING WITH TWO TYPES OF PERFORATED COATINGS, SUBJECTED TO DIAMETRAL COMPRESSION

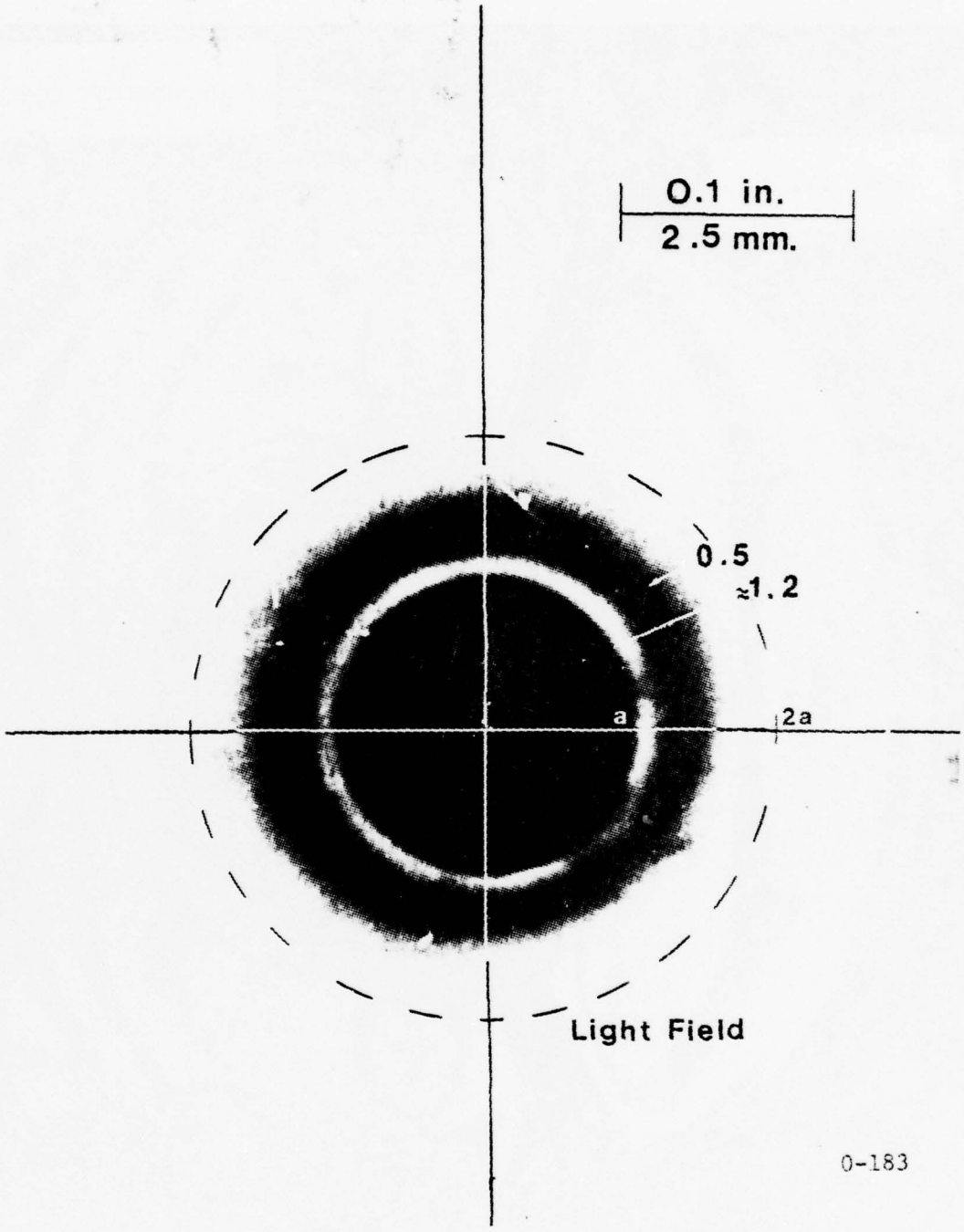

FIG. 4 ISOCHROMATICS ASSOCIATED WITH RESIDUAL STRESSES, AROUND A HOLE IN A COATING, LOCATED AT A DISTANCE ($r/b = 0.61$) FROM THE CENTER OF A CIRCULAR RING

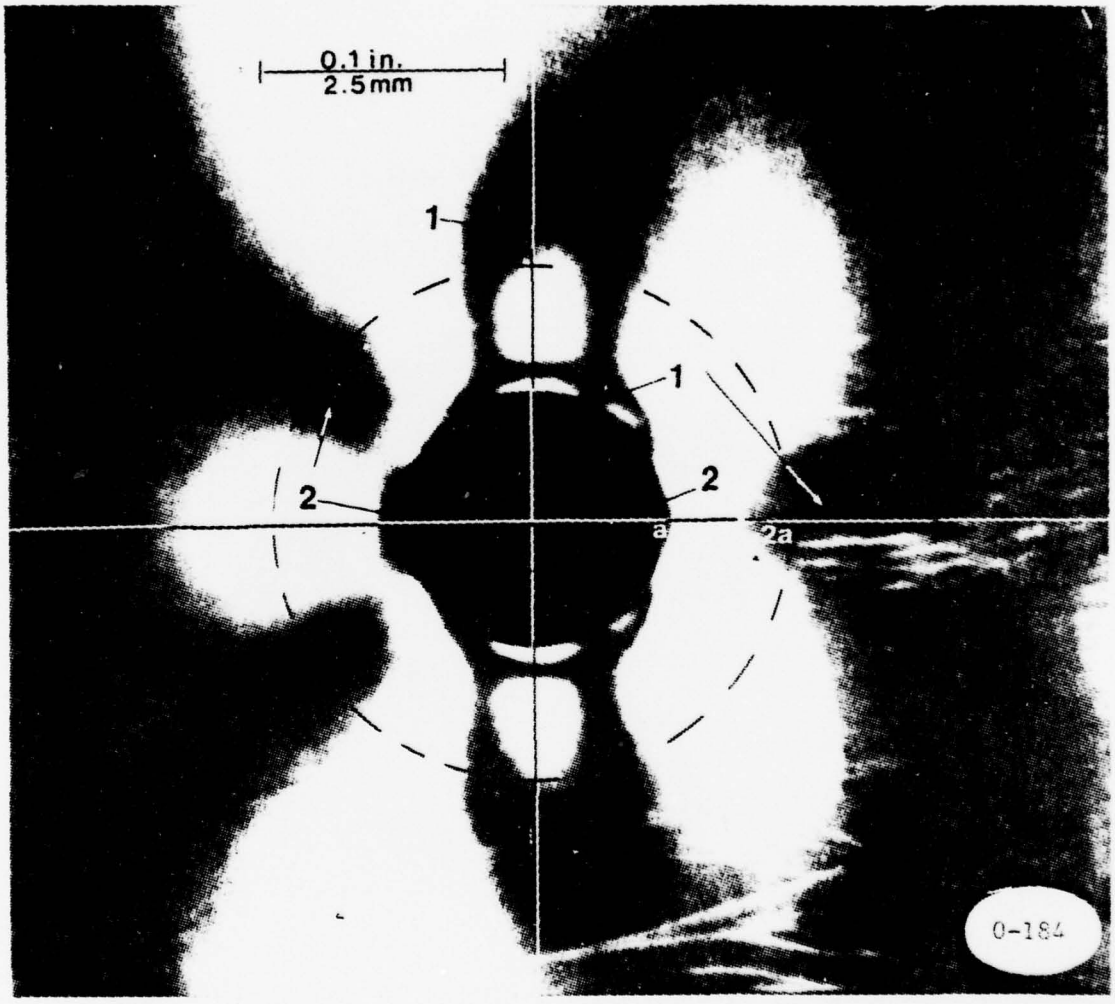

FIG. 5 ISOCHROMATICS AROUND A HOLE IN A COATING, ON THE HORIZONTAL AXIS ($r/b = 0.61$) OF A CIRCULAR RING SUBJECTED TO VERTICAL COMPRESSION (DARK FIELD)

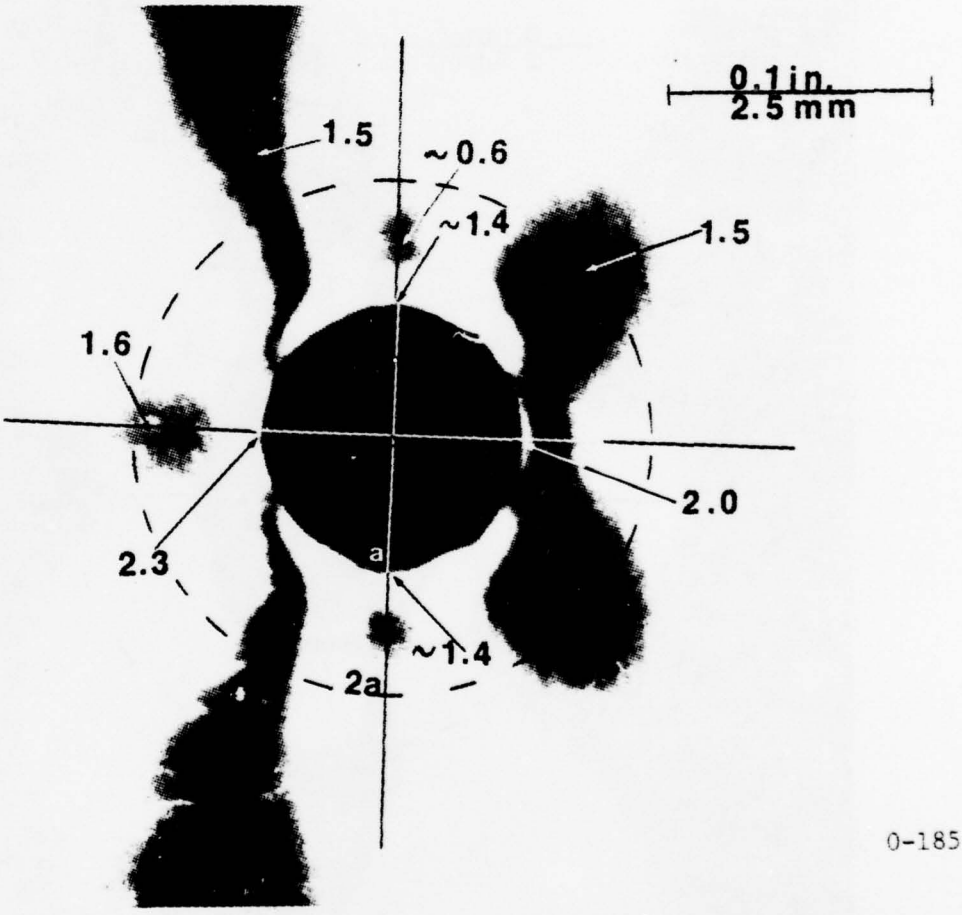

FIG. 6 ISOCHROMATICS AROUND A HOLE, IN A COATING ON THE HORIZONTAL AXIS ($r/b = 0.61$) OF A CIRCULAR RING SUBJECTED TO VERTICAL COMPRESSION (LIGHT FIELD)

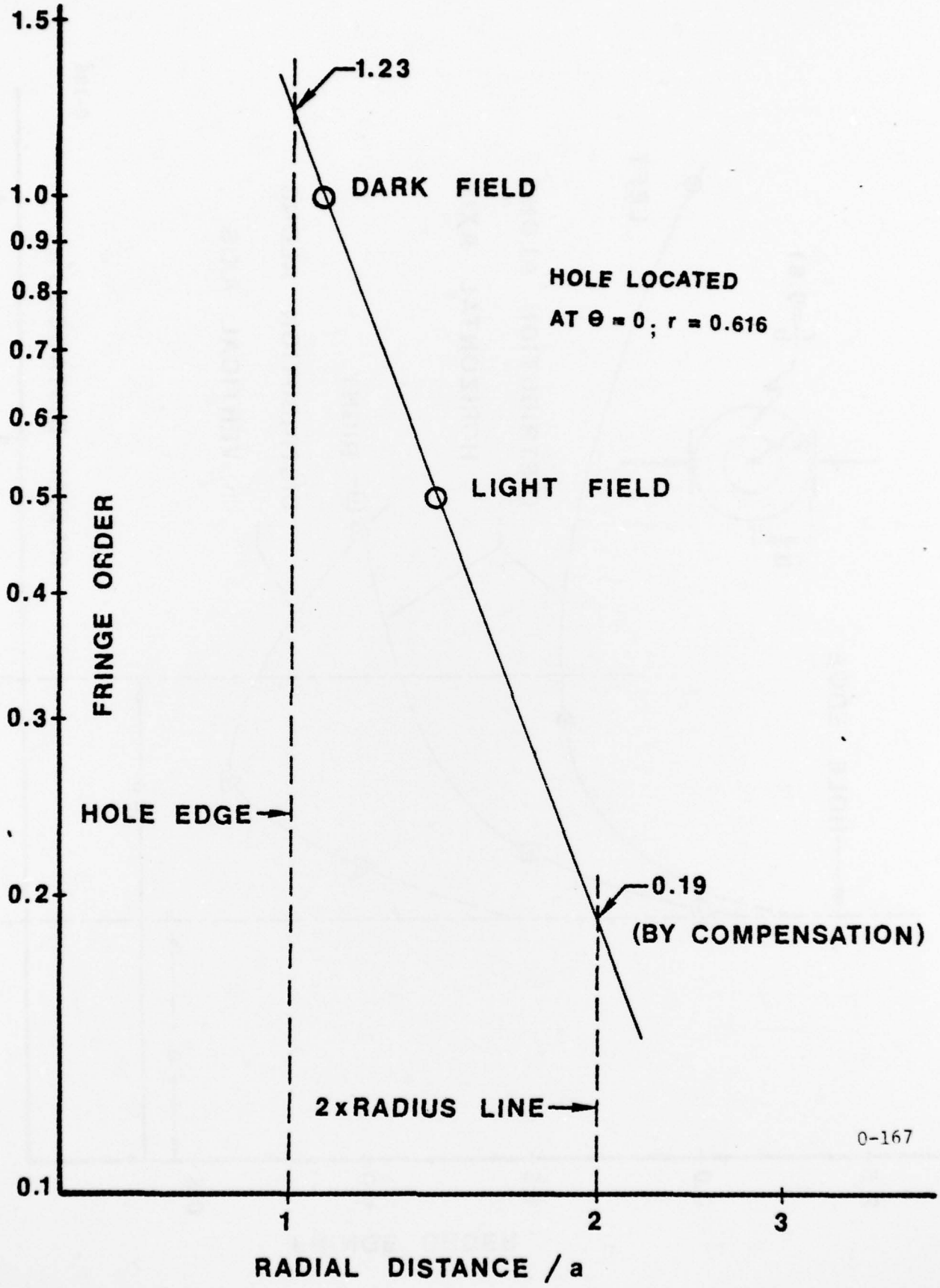

FIG. 7 RESIDUAL STRESS DISTRIBUTION AROUND A HOLE IN THE COATING ON A CIRCULAR RING (LOG-LOG PLOT)

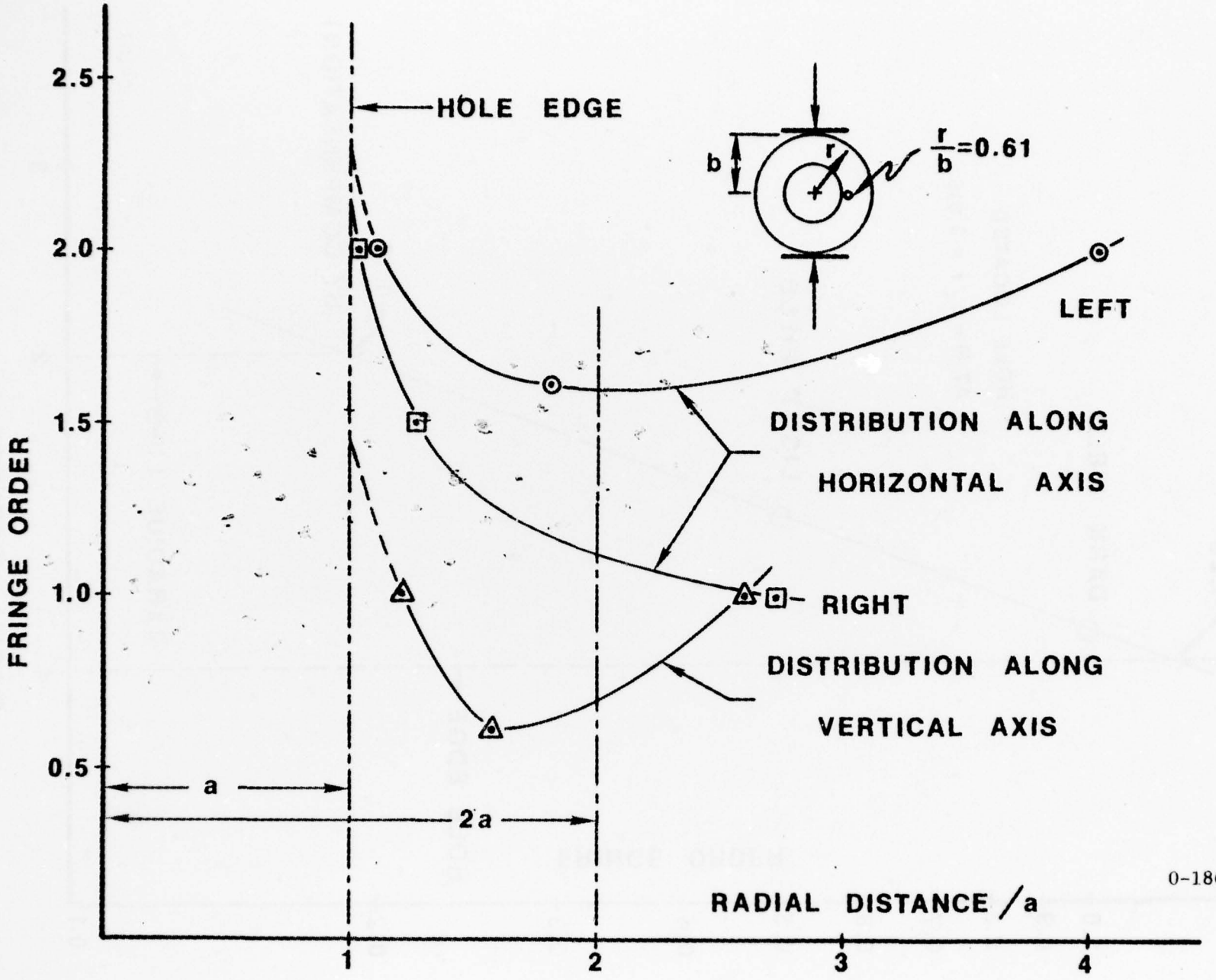

FIG. 8 FRINGE ORDERS ON THE AXES OF SYMMETRY OF A HOLE IN THE COATING, ON THE HORIZONTAL AXIS ($r/b = 0.61$) OF A CIRCULAR RING SUBJECTED TO VERTICAL COMPRESSION

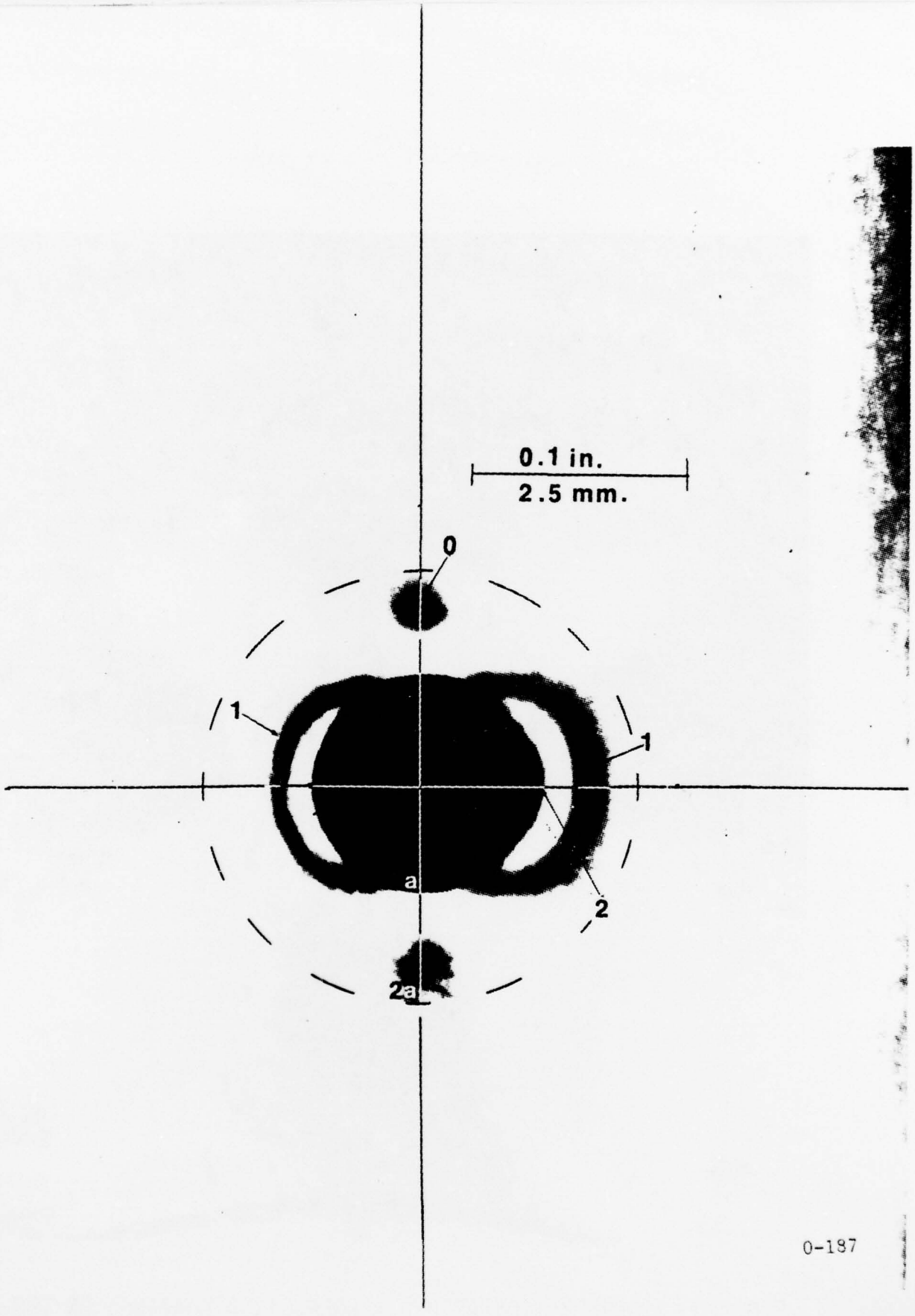

FIG. 9 ISOCHROMATICS AROUND A HOLE IN A COATING ON THE HORIZONTAL AXIS ($r/b = 0.61$) OF A CIRCULAR RING SUBJECTED TO VERTICAL COMPRESSION (DARK FIELD)

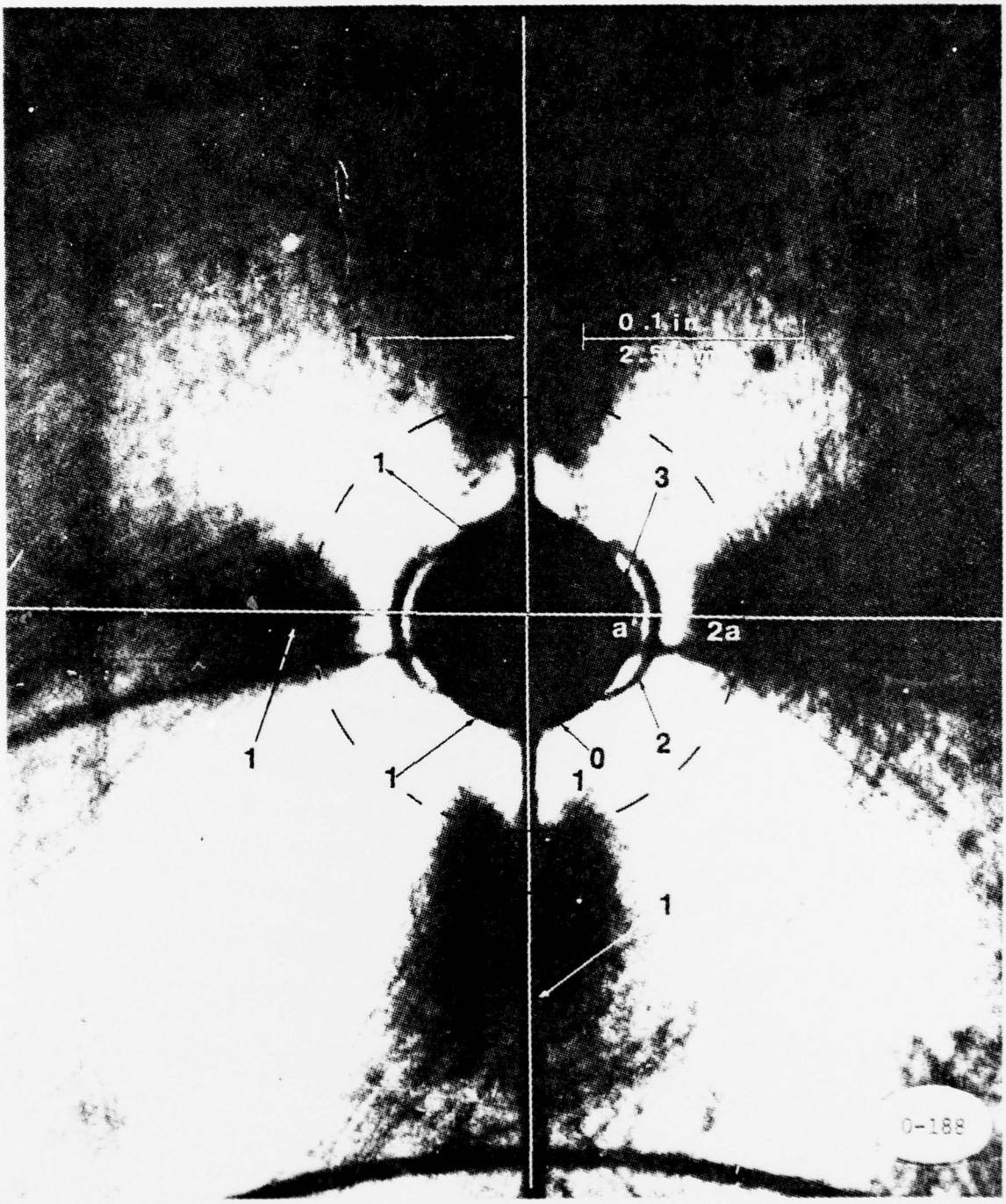

FIG. 10 ISOCHROMATICS AROUND A HOLE, IN A COATING, ON THE VERTICAL AXIS ($r/b = 0.61$) OF A CIRCULAR DISK SUBJECTED TO VERTICAL COMPRESSION (DARK FIELD)

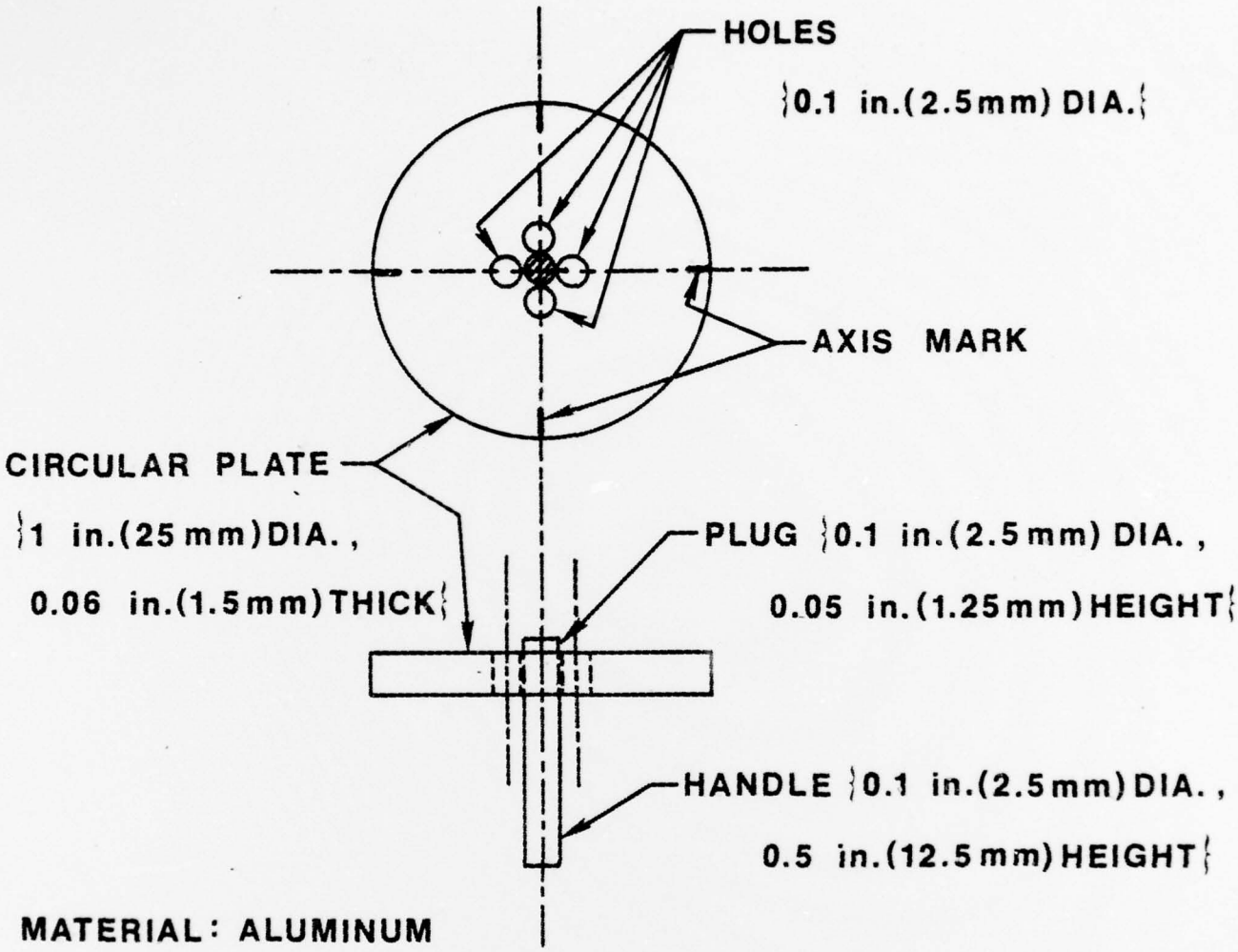

0-168

FIG. 11 DEVICE FOR LOCATION OF POINTS ON TWO AXES OF SYMMETRY AROUND THE HOLE IN THE COATING

ONR DISTRIBUTION LIST

Government

Office of Naval Research
Department of the Navy
Arlington, VA 22217
Attn: Code 474 (2)

Office of Naval Research
Department of the Navy
Arlington, VA 22217
Attn: Code 471 (2)

Office of Naval Research
Department of the Navy
Arlington, VA 22217
Attn: Code 200 (2)

Director
ONR Branch Office
666 Summer Street
Boston, MA 02210

Director
ONR Branch Office
536 South Clark Street
Chicago, IL 60605

Director
ONR - New York Area Office
715 Broadway - 5th Floor
New York, NY 10003

Director
ONR Branch Office
1030 East Green Street
Pasadena, CA 91106

Naval Research Laboratory (6)
Code 2627
Washington, D.C. 20375

Defense Documentation Center
Cameron Station (12)
Alexandria, VA 22314

NAVY

Undersea Explosion Res. Division
Naval Ship Research & Development Center-Att. E Palmer 177
Norfolk Naval Shipyard
Portsmouth VA 23709

Naval Research Laboratory
Washington, D.C. 20375
Attn: Code 8400

Naval Research Laboratory
Washington, D.C. 20375
Attn: Code 8410

Naval Research Laboratory
Washington, D.C. 20375
Attn: Code 8430

Naval Research Laboratory
Washington, D.C. 20375
Attn: Code 8440

Naval Research Laboratory
Washington, D.C. 20375
Attn: Code 6300

Naval Research Laboratory
Washington, D.C. 20375
Attn: Code 6390

Naval Research Laboratory
Washington, D.C. 20375
Attn: Code 6380

David W. Taylor Naval Ship
Research & Development Center
Annapolis, MD 21402
Attn: Code 2740

David W. Taylor Naval Ship
Research & Development Center
Annapolis, MD 21402
Attn: Code 28

David W. Taylor Naval Ship
Research & Development Center
Annapolis, MD 21402
Attn: Code 281

U.S. Naval Weapons Center
China Lake, CA 93555
Attn: Code 4062

U.S. Naval Weapons Center
China Lake, CA 93555
Attn: Code 4520

Commanding Officer
U.S. Naval Civil Eng. Lab.
Code L31
Port Hueneme, CA 93041

Naval Surface Weapons Center
White Oak
Silver Spring, MD 20910
Attn: Code R-10

Naval Surface Weapons Center
White Oak
Silver Spring, MD 20910
Attn: Code G-402

Naval Surface Weapons Center
White Oak
Silver Spring, MD 20910
Attn: Code K-82

Technical Director
Naval Ocean Systems Center
San Diego, CA 92152

Supervisor of Shipbuilding
U.S. Navy
Newport News, VA 23607

U.S. Navy Underwater Sound
Reference Division
Naval Research Laboratory
P.O. Box 8337
Orlando, FL 32806

Chief of Naval Operations
Department of the Navy
Washington, DC 20350
Attn: Code OP-098

Strategic Systems Project Off.
Department of the Navy
Washington, DC 20376
Attn: NSP-200

Naval Air Systems Command
Department of the Navy
Washington, DC 20361
Attn: Code 5302

Naval Air Systems Command
Department of the Navy
Washington, DC 20361
Attn: Code 604

Naval Air Systems Command
Department of the Navy
Washington, DC 20361
Attn: Code 320B

Naval Air Development Center
Director, Aerospace Mechanics
Warminster, PA 18974

U.S. Naval Academy
Engineering Department
Annapolis, MD 21402

Naval Facilities Eng. Command
200 Stovall Street
Alexandria, VA 22332
Attn: Code 03 (Res. & Devel.)

Naval Facilities Engr. Command
200 Stovall Street
Alexandria, VA 22332
Attn: Code 04B

Naval Facilities Engr. Command
200 Stovall Street
Alexandria, VA 22332
Attn: Code 045

Naval Facilities Engr. Command
200 Stovall Street
Alexandria, VA 22332
Attn: Code 14114 (Tech. Lib.)

Naval Sea Systems Command
Department of the Navy
Washington, DC 20362
Attn: Code 03 (Res. & Tech.)

Naval Sea Systems Command
Department of the Navy
Washington, DC 20362
Attn: Code 037

Naval Sea Systems Command
Department of the Navy
Washington, DC 20362
Attn: Code 035

Naval Ship Engineering Center
Department of the Navy
Washington, DC 20362
Attn: Code 6105G

Naval Ship Engineering Center
Department of the Navy
Washington, DC 20362
Attn: 6114

Naval Ship Engineering Center
Department of the Navy
Washington, DC 20362
Attn: 6120D

Naval Ship Engineering Center
Department of the Navy
Washington, DC 20362
Attn: Code 6128

Naval Ship Engineering Center
Department of the Navy
Washington, DC 20362
Attn: Code 6129

Commanding Officer & Director
David W. Taylor Naval Ship
Research & Development Center
Bethesda, MD 20084
Attn: Code 042

Commanding Officer & Director
David W. Taylor Naval Ship
Research & Development Center
Bethesda, MD 20084
Attn: Code 17

Commanding Officer & Director
David W. Taylor Naval Ship
Research & Development Center
Bethesda, MD 20084
Attn: Code 172

Commanding Officer & Director
David W. Taylor Naval Ship
Research & Development Center
Bethesda, MD 20084
Attn: Code 173

Commanding Officer & Director
David W. Taylor Naval Ship
Research & Development Center
Bethesda, MD 20084
Attn: Code 174

Commanding Officer & Director
David W. Taylor Naval Ship
Research & Development Center
Bethesda, MD 20074
Attn: Code 1800

Commanding Officer & Director
David W. Taylor Naval Ship
Research & Development Center
Bethesda, MD 20084
Attn: Code 1844

Commanding Officer & Director
David W. Taylor Naval Ship
Research & Development Center
Bethesda, MD 20084
Attn: Code 1102.1

Commanding Officer & Director
David W. Taylor Naval Ship
Research & Development Center
Bethesda, MD 20084
Attn: Code 1900

Commanding Officer & Director
David W. Taylor Naval Ship
Research & Development Center
Bethesda, MD 20084
Attn: Code 1901

Commanding Officer & Director
David W. Taylor Naval Ship
Research & Development Center
Bethesda, MD 20084
Attn: Code 1945

Commanding Officer & Director
David W. Taylor Naval Ship
Research & Development Center
Bethesda, MD 20084
Attn: Code 1960

Commanding Officer & Director
David W. Taylor Naval Ship
Research & Development Center
Bethesda, MD 20084
Attn: 1962

Naval Underwater Systems Center
Newport, RI 02840
Attn: Dr. R. Trainor

Naval Surface Weapons Center
Dahlgren Laboratory
Dahlgren, VA 22448
Attn: Code G04

Naval Surface Weapons Center
Dahlgren Laboratory
Dahlgren, VA 22448
Attn: Code G20

Technical Director
Mare Island Naval Shipyard
Vallejo, CA 94592

U.S. Naval Postgraduate School
Library
Code 0384
Monterey, CA 93940

Webb Institute of Naval
Architecture- Attn: Librarian
Crescent Beach Road, Glen Cove
Long Island, NY 11542

Commanding Officer (2)
U.S. Army Research Office
P.O. Box 12211
Research Triangle PK. NC 27709
Attn: J. J. Murray, CRD-AA-IP

Watervliet Arsenal
MAGGS Research Center
Watervliet, NY 12189
Attn: Director of Research

U.S. Army Materials and
Mechanics Research Center
Watertown, MA 02172
Attn: Dr. R. Shea DRXMR-T

U.S. Army Missile Research and
Development Center
Redstone Scientific Info. Cen.
Chief, Document Section
Redston Arsenal, AL 35809

Army Research & Development
Center
Fort Belvoir, VA 22060

NASA
Structures Research Division
Langley Research Center
Langley Station
Hampton, VA 23365

NASA
Associate Adm. for Advanced
Research & Technology
Washington, DC 20546

Scientific & Tech. Info. Fac.
NASA Representative (S-AK/DL)
P.O. Box 5700
Bethesda, MD 20014

Commander WADD
Wright Patterson AFB
Attn: Code WXRMDD
Dayton, OH 45433

Commander WADD
Wright Patterson AFB
Attn: Code AFFDL(FDDS)
Dayton, Oh 45433

Commander WADD
Wright Patterson AFB
Attn: Structures Div.
Dayton, OH 45433

Commander WADD
Wright Patterson AFB
Attn: Code AFLC (MCEEA)
Dayton, OH 45433

Chief Appl.Mechanics Group
U.S. Air Force Inst. of Tech.
Wright-Patterson AFB
Dayton, OH 45433

Chief, Civil Engr. Branch
WLRC, Research Division
Air Force Weapons Laboratory
Kirtland AFB, Albuquerque, NM
87117

Air Force Office of Scientific
Research
Bolling Air Force Base
Washington, DC 20332
Attn: Mechanics Div.

Department of the Air Force
Air University Library
Maxwell Air Force Base
Montgomery, AL 36112

Commandant
Chief, Testing & Devel. Div.
U.S. Coast Guard
1300 E Street, NW
Washington, D.C 20226

Technical Director
Marine Corps Devl. & Educ.
Command
Quantico, VA 22134

Director Defense Research & Egr.
Technical Lib. Rm 3C-128
The Pentagon
Washington, D.C. 20301

Director
National Bureau of Standards
Washington, DC 20034
Attn: B. L. Wilson, EM 219

Dr. M. Caus
National Science Foundation
Environmental REsearch Div.
Washington, DC 20550

Library of Congress
Science & Technology Div.
Washington, DC 20540

Director
Defense Nuclear Agency
Washington, DC 20305
Attn: SPSS

Mr. Jerome Persh
Staff Specialist for Materials
and Structures
OUSDR&E, The Pentagon-Rm 3D1089
Washington, DC 20301

Chief, Airframe & Equipment
Branch - FS-120
Office of Flight Standards
Federal Aviation Agency
Washington, DC 20553

National Academy of Sciences
National Research Council
Ship Hull Research Committee
2101 Constitution Avenue
Washington, DC 20418(A.R.Lytle)

National Science Foundation
Engineering Mechanics Section
Division of Engineering
Washington, DC 20550

Picatinny Arsenal
Plastics Tech. Evaluation Center
Attn: Technical Info. Section
Dover, NJ 07801

Maritime Administration
Office of Maritime Technology
14th & Constitution Ave., NW
Washington, DC 20230

Maritime Administration
Office of Ship Construction
14th & Constitution AVE., NW
Washington, DC 20230

Dr. H. H. Vanderveldt
Dept. of the Navy
Naval Sea Systems-Code 03522
Washington, D.C. 20362

UNIVERSITIES

Dr. J. Tinsley Oden
University of Texas at Austin
345 Engr. Science Building
Austin, TX 78712

Professor Walter D. Pilkey
University of Virginia
Res. Lab. for Egr. Sciences
School of Egr. & Appl. Sciences
Charlottesville, VA 22901

Professor Albert I. King
Wayne State University
Biomechanics Research Center
Detroit, MI 48202

Prof. Julius Miklowitz
California Inst. of Technology
Div. of Engr. & Appl Science
Pasadena, CA 91109

Professor K. D. Willmert
Clarkson College of Technology
Dept. of Mechanical Engineering
Potsdam, NY 13676

Dr. V. R. Hodgson
Wayne State University
School of Medicine
Detroit, MI 48202

Dr. Harold Liebowitz, Dean
School of Engr. & Appl. Science
George Washington University
Washington, DC 20052

Dr. Walter E. Haisler
Texas A&M University
Aerospace Engineering Department
College Station, TX 77843

Dean B. A. Boley
Northwestern University
Department of Civil Engineering
Evanston, IL 60201

Professor Eli Sternberg
California Inst. of Technology
Div. of Engr. & Appl. Science
Pasadena, CA 91109

Dr. Hussein A. Kamel
University of Arizona
Dept. of Aero. & Mechanical Egr.
Tucson, AZ 85721

Professor P. G. Hodge, Jr.
University of Minnesota
Dept. of Aero. Egr. & Mech.
Minneapolis, MN 55455

Professor Paul M. Naghdi
University of California
Dept. of Mechanical Engr.
Berkeley, CA 94720

Dr. S. J. Fenves
Carnegie-Mellon University
Dept. of Civil Engineering
Schenley Park
Pittsburgh, PA 15213

Dr. D. C. Drucker
University of Illinois
Dean of Engineering
Urbana, IL 61801

Professor F. L. DiMaggio
Columbia University
Dept. of Civil Engineering
New York, NY 10027

Dr. Ronald L. Huston
Dept. of Engineering Analysis
University of Cincinnati
Cincinnati, OH 45221

Professor N. M. Newmark
University of Illinois
Department of Civil Engineering
Urbana, IL 61803

Professor Norman Jones
MIT
Dept. of Ocean Engineering
Cambridge, MA 02139

Prof. G. C. M. Sih
Lehigh University
Inst. of Fracture & Solid Mech.
Bethlehem, PA 18015

Professor E. Reissner
Univ. of California, San Diego
Dept. of Applied Mechanics
La Jolla, CA 92037

Prof. E. J. Skudrzyk
Pennsylvania State University
Applied Research Laboratory
Department of Physics
State College, PA 16801

Prof. Albert S. Kobayashi
University of Washington
Dept. of Mechanical Engineering
Seattle, WA 98105

Professor William A. Nash
University of Massachusetts
Dept. of Mech. & Aero. Egr.
Amherst, MA 01002

Professor J. Kempner
Polytechnic Inst. of New York
Dept. of Aero.Egr.,Appl.Mech
333 Jay Street
Brooklyn, NY 11201

Professor Daniel Frederick
Virginia Polytechnic Inst. &
State University
Dept. of Engineering Mechanics
Blacksburg, VA 24061

Professor G. Herrmann
Stanford University
Dept. of Applied Mechanics
Stanford, CA 94305

Professor J. Klosner
Polytechnic Inst. of New York
Dept. of Aero.EGR., Appl.Mech.
333 Jay Street
Brooklyn, NY 11201

Professor A. C. Eringen
Princeton University
Dept. of Aero. & Mechanical Sci.
Princeton, NJ 08540

Professor J. D. Achenbach
Northwestern University
Dept. of Civil Engineering
Evanston, IL 60201

Professor R. A. Schapery
Texas A&M University
Dept. of Civil Engineering
College Station, TX 77843

Professor E. H. Lee
Stanford University
Div. of Engineering Mechanics
Stanford, CA 94305

Professor S. B. Dong
University of California
Dept. of Mechanics
Los Angeles, CA 90024

Professor Burt Paul
University of Pennsylvania
Towne School of Civil and
Mechanical Engineering
Philadelphia, PA 19104

Professor H. W. Liu
Syracuse University
Dept. of Chemical EGR & Metal.
Syracuse, NY 13210

Professor S. Bodner
Technion R & D Foundation
Haifa, Israel

Professor Werner Goldsmith
University of California
Department of Mech. Engr.
Berkeley, CA 94720

Professor R. S. Rivilin
Lehigh University
Center for Appl. of Math.
Bethlehem, PA 18015

Professor F. A. Cozzarelli
SUNY at Buffalo
Div. of Inter. Studies
Karr Parker Egr. Bldg.
Buffalo, NY 14214

Professor Joseph L. Rose
Drexel University
Dept. of Mech. Egr. & Mech.
Philadelphia, PA 19104

Professor B. K. Donaldson
University of Maryland
Aerospace Engineering Dept.
College Park, MD 20742

Professor Joseph V. Clark
Catholic University of America
Dept. of Mechanical Engr.
Washington, DC 20064

Professor T. C. Huang
University of Wisc.-Madison
Dept. of Eng. Mechanics
Madison, WI 53706

Professor Isaac Fried
Boston University
Dept. of Mathematics
Boston, MA 02215

Dr. Samuel B. Batdorf
University of California
School of Engr.&Appl. Science
Los Angeles, CA 90024

Professor Michael Pappas
New Jersey Inst. of Technology
Newark College of Engineering
323 High Street
Newark, NJ 07102

Professor E. Krempl
Rensselaer Polytechnic Inst.
Division of Engineering
Engineering Mechanics
Troy, NY 12181

Dr. Jack R. Vinson
University of Delaware
Dept. of Mech & Aero. Engr.
and Center for Composite Matls.
Newark, DL 19711

Dr. Dennis A. Nagy
Princeton University.
School of Engr. & Appl. Science
Dept. of Civil Engineering
Princeton, NJ 08540

Dr. J. Duffy
Brown University
Division of Engineering
Providence, RI 02912

Dr. J. L. Swedlow
Carnegie-Mellon University
Dept. of Mechanical Engineering
Pittsburgh, PA 15213

Dr. V. K. Varadan
Ohio State Un.Res. Foundation
Dept. of Engineering Mechanics
Columbus, OH 43210

Dr. Jackson C. S. Yang
University of Maryland
Dept. of Mechanical Engineering
College Park, MD 20742

Dr. Z. Hashin
University of Pennsylvania
Dept. of Metallurgy & Mats. Sci.
College Of Engr. & Appl. Sci
Philadelphia, PA 19104

Dr. T. Y. Chang
University of Akron
Department of Civil Engineering
Akron, OH 44325

Professor Charles W. Bert
University of Oklahoma
School of Aerospace., Mechanical
and Nuclear Engineering
Norman, OK 73019

Professor Satya N. Atluri
Georgia Inst. of Technology
School of Egr. Sci & Mech.
Atlanta, GA 30332

Professor Graham F. Carey
University of Texas at Austin
Dept. of Aero. Egr. & Egr.Mech.
Austin, TX 78712

Dr. Jackson C. S. Yang
Advanced Tech. & Research, Inc.
10006 Green Forest Drive
Adelphi, MD 20783

Dr. Norman Hobbs
Kaman AviDyne
Division of Kaman Sci. Corp.
Burlington, MA 01803

Argonne National Laboratory
Library Services Department
9700 South Cass Avenue
Argonne, IL 60440

Dr. M. C. Junger
Cambridge Acoustical Assoc.
1033 Massachusetts Avenue
Cambridge, MA 02138

Dr. V. Godino
General Dynamics Corporation
Electric Boat Division
Groton, CT 06340

Dr. J. E. Greenspon
J.G. Engineering Research Assoc.
3831 Menlo Drive
Baltimore, MD 21215

Dr. K. C. Park
Lockheed Missile & Space Co.
3251 Hanover Street
Palo Alto, CA 94304

Newport News Shipbuilding and
Dry Dock Company
Library
Newport News, VA 23607

Dr. J. F. Bozich
McDonnell Douglas Corp.
5301 Bolsa Avenue
Huntington Beach, CA 92647

Dr. H. N. Abramson
Southwest Research Institute
8500 Culebra Road
San Antonio, TX 78284

Dr. R. C. DeHart
Southwest Research Institute
8500 Culebra Road
San Antonio, TX 78284

Dr. M. L. Baron
Wiedlinger Associates
110 East 59th Street
New York, NY 10022

Dr. T. L. Geers
Lockheed Missiles & Space Co.
3251 Hanover Street
Palo Alto, CA 94304

Mr. William Caywood
Applied Physics Laboratory
Johns Hopkins Road
Laurel, MD 20810

Dr. Robert E. Nickell
Pacifica Technology
P.O. Box 148
Del Mar, CA 92014

Dr. M. F. Kanninen
Battelle Columbus Labs.
505 King Avenue
Columbus, OH 43201

Dr. G. T. Hahn
Battelle Columbus Labs.
505 King Avenue
Columbus, OH 43201

Dr. A. A. Hochrein
Dahlgren Associates, Inc.
Springlake Research Center
15110 Frederick Road
Woodbine, MD 21797

Mr. Richard Y. Dow
National Academy of Sciences
2101 Constitution Avenue
Washington, DC 20418

Mr. H. L. Kington
Airesearch Mfg. Co. of Arizona
P.O. Box 5217
111 South 34th Street
Phoenix, AZ 85010

Dr. M. H. Rice
Systems, Science & Software
P.O. Box 1620
La Jolla, CA 92037

SECURITY CLASSIFICATION OF THIS PAGE (When Data Entered)

REPORT DOCUMENTATION PAGE

READ INSTRUCTIONS BEFORE COMPLETING FORM

1. REPORT NUMBER: 51
2. GOVT ACCESSION NO.:
3. RECIPIENT'S CATALOG NUMBER:

4. TITLE (and Subtitle): DETERMINATION OF STRAINS IN PHOTOELASTIC COATINGS

5. TYPE OF REPORT & PERIOD COVERED:

6. PERFORMING ORG. REPORT NUMBER:

7. AUTHOR(s): A. J. Durelli and K. Rajaiah

8. CONTRACT OR GRANT NUMBER(s):

9. PERFORMING ORGANIZATION NAME AND ADDRESS:
Oakland University
Rochester, MI 48063
405 252

10. PROGRAM ELEMENT, PROJECT, TASK AREA & WORK UNIT NUMBERS:

11. CONTROLLING OFFICE NAME AND ADDRESS:
Office of Naval Research
Department of the Navy
Washing, D.C. 20025

12. REPORT DATE: April 1979

13. NUMBER OF PAGES: 47

14. MONITORING AGENCY NAME & ADDRESS(if different from Controlling Office):

15. SECURITY CLASS. (of this report): Unclassified

15a. DECLASSIFICATION/DOWNGRADING SCHEDULE:

16. DISTRIBUTION STATEMENT (of this Report):
Distribution of this Report is unlimited

17. DISTRIBUTION STATEMENT (of the abstract entered in Block 20, if different from Report):

18. SUPPLEMENTARY NOTES:

19. KEY WORDS (Continue on reverse side if necessary and identify by block number):
Hole Method
Photoelastic coating
Separation of stresses
Coating stresses
Reflection polariscope

20. ABSTRACT (Continue on reverse side if necessary and identify by block number):
Photoelastic coatings can be cemented directly to actual structural components and tested under field conditions. This important advantage has made them relatively popular in industry. The information obtained, however, may be misinterpreted and lead to serious errors. A correct interpretation requires the separation of the principal strains and so far, this operation has been found very difficult. Following a previous

DD FORM 1 JAN 73 1473 EDITION OF 1 NOV 65 IS OBSOLETE
S/N 0102-014-6601 |

SECURITY CLASSIFICATION OF THIS PAGE (When Data Entered)

paper by one of the authors, it is proposed to drill small holes in the in the coating and record the birefringence at points removed from the edge of the holes. The theoretical background of the method is reviewed; the technique necessary to use it is explained and two applications are described. The precision of the method is evaluated and found satisfactory in contradiction to information previously published in the literature.